



International Institute for
Applied Systems Analysis
Schlossplatz 1
A-2361 Laxenburg, Austria

Tel: +43 2236 807 342
Fax: +43 2236 71313
E-mail: publications@iiasa.ac.at
Web: www.iiasa.ac.at

Interim Report

IR-13-075

**Single-gene speciation with pleiotropy:
Effects of allele dominance population size and delayed
inheritance**

Masato Yamamichi
Akira Sasaki (sasaki@iiasa.ac.at)

Approved by

Ulf Dieckmann
Director, Evolution and Ecology Program

June 2015

Interim Reports on work of the International Institute for Applied Systems Analysis receive only limited review. Views or opinions expressed herein do not necessarily represent those of the Institute, its National Member Organizations, or other organizations supporting the work.

2 **Single-gene speciation with pleiotropy:**
3 **Effects of allele dominance, population size, and delayed**
4 **inheritance**

5
6
7 Masato Yamamichi*¹, Akira Sasaki^{¶2,3}

8 1) Department of Ecology and Evolutionary Biology, Cornell University, Ithaca, NY 14853,
9 USA

10 2) Department of Evolutionary Studies of Biosystems, Graduate University for Advanced
11 Studies (Sokendai), Hayama, Kanagawa, 240-0193, Japan

12 3) Evolution and Ecology Program, International Institute for Applied System Analysis,
13 A-2361, Laxenburg, Austria

14 *corresponding author: my287@cornell.edu, Phone: +1-607-254-4231

15 ¶: sasaki_akira@soken.ac.jp, Phone: +81-46-858-1537

16
17 Running Title: single-gene speciation with pleiotropy

18 Key Words: ecological speciation, magic trait, positive frequency-dependent selection,
19 maternal effect, fixation probability, speciation gene

20
21 **Figures 1, 2, 3, 4 (color), 5 (color), & 6; Table 1**

22 **Supporting information: 8 appendices with 1 supplement table & 6 supplement figures**

23 **No. of words in the main text: 5520**

24 **ABSTRACT**

25 Single-gene speciation is considered to be unlikely, but an excellent example is found in land
26 snails, in which a gene for left-right reversal has given rise to new species multiple times.
27 This reversal might be facilitated by their small population sizes and maternal effect (i.e.,
28 ‘delayed inheritance’, in which an individual’s phenotype is determined by the genotype of its
29 mother). Recent evidence suggests that a pleiotropic effect of the speciation gene on
30 anti-predator survival may also promote speciation. Here we theoretically demonstrate that,
31 without a pleiotropic effect, in small populations the fixation probability of a recessive mutant
32 is higher than a dominant mutant, but they are identical for large populations and sufficiently
33 weak selection. With a pleiotropic effect that increases mutant viability, a *dominant* mutant
34 has a higher fixation probability if the strength of viability selection is sufficiently greater
35 than that of reproductive isolation, whereas a *recessive* mutant has a higher fixation
36 probability otherwise. Delayed inheritance increases the fixation probability of a mutant if
37 viability selection is weaker than reproductive isolation. Our results clarify the conflicting
38 effects of viability selection and positive frequency-dependent selection due to reproductive
39 isolation and provide a new perspective to single-gene speciation theory.

40 INTRODUCTION

41 Ever since Darwin, understanding the genetic and ecological conditions under which
42 speciation occurs has been an ongoing challenge in evolutionary biology (Coyne and Orr
43 2004). One longstanding issue of debate in speciation theory concerns the number of genes
44 that are necessary for speciation to occur. Under the classic Bateson-Dobzhansky-Muller
45 (BDM) model, speciation requires changes in at least two genes because if there is one new
46 allele with strong effects on heterozygote viability or mating compatibility but without
47 epistasis to other genes, then the fitness of variants that harbor that allele should decrease,
48 making the fixation of this allele in the population difficult. In contrast, negative epistatic
49 interactions between independently derived alleles (A and B) at two loci can establish
50 reproductive isolation between descendant genotypes (AA bb and aaBB) without reproductive
51 isolation between the ancestral genotype (aabb) and daughter lineages (Bateson 1909;
52 Dobzhansky 1936; Muller 1942).

53 Although the classical BDM incompatibility model has been influential in
54 explaining the speciation process (Orr 1996; Gavrillets 2004; Bank et al. 2012), the model
55 cannot explain the evolution of reproductive isolation via a single gene. Speciation that results
56 from genetic substitution at a single locus is known as ‘single-gene speciation’ (Orr 1991).

57 Single-gene speciation has been of special interest for the following reasons: (1) “one-locus
58 models are a natural starting point for theoretical approaches to many evolutionary
59 phenomena” (Gavrilets 2004); (2) there are several examples of empirical evidence for the
60 determination of mating traits by a single-locus (see Gavrilets 2004; Servedio et al. 2011 for
61 review); and (3) a single speciation gene that pleiotropically contributes to reproductive
62 isolation and divergent adaptation through a single trait ('automatic magic trait' according to
63 Servedio et al. 2011) or several traits (Slatkin 1982) has been thought to promote ecological
64 speciation (Rundle and Nosil 2005). Speciation becomes less probable if one locus is
65 responsible for ecological adaptation and another locus is responsible for reproductive
66 isolation because recombination breaks down the association between the two loci
67 (Felsenstein 1981). Here, we refer to this dual function of a single gene as pleiotropic effects
68 or simply pleiotropy (Slatkin 1982). In spite of these longstanding interests and an increasing
69 number of studies that suggests the involvement of adaptation in speciation (Schluter 2009),
70 the theoretical framework to explain the process of single-gene speciation is not robust
71 because previous studies have relied heavily on numerical simulations (Kirkpatrick and
72 Ravigné 2002; Gavrilets 2004). In this paper, we use new analytical results to investigate the
73 effects of pleiotropy, allele dominance, population size, and maternal effect on the fixation

74 process of the speciation gene in single-gene speciation.

75 An excellent example of single-gene speciation is found in land snails (see
76 Schilthuizen and Davison 2005; Okumura et al. 2008 for review). Handedness is shown to be
77 controlled by two alleles at a single nuclear locus in phylogenetically segregated families of
78 pulmonate snails (Boycott et al. 1930; Degner 1952; Murray and Clarke 1976; Freeman and
79 Lundelius 1982; Ueshima and Asami 2003), and mating between opposite coiling individuals
80 rarely occurs (Johnson 1982; Gittenberger 1988; Asami et al. 1998). Thus, the handedness
81 gene is responsible for pre-mating isolation. Despite the positive frequency-dependent
82 selection against rare mutants predicted by the BDM model (Johnson 1982; Asami et al.
83 1998), it has been shown that evolutionary transitions from an abundant dextral (clockwise
84 coiling) species to a mutant sinistral (counter-clockwise coiling) species have occurred
85 multiple times (Ueshima and Asami 2003; Davison et al. 2005; Hosono et al. 2010; Gittenberger
86 et al. 2012).

87 Why is single-gene speciation possible in snails? Following Gittenberger (1988),
88 Orr (1991) proposed that small population sizes and maternal effect (i.e., delayed inheritance:
89 Fig. 1) in snail populations could promote single-gene speciation. Because snails have low
90 mobility, local populations tend to be isolated from one another, which causes repeated

91 extinction and colonization events. Consequently, the effective population sizes of snails are
92 small and genetic drift is strong (Arnaud and Laval 2004; Hosono 2012). Delayed inheritance of
93 handedness is a type of maternal effect in which an individual's phenotype is determined by
94 the genotype of its mother (Fig. 1: Boycott et al. 1930; Degner 1952; Murray and Clarke
95 1976; Freeman and Lundelius 1982). Subsequent theoretical studies on the evolution of snail
96 coiling have basically attributed the cause of single-gene speciation to these two factors (van
97 Batenburg and Gittenberger 1996; Stone and Björklund 2002; but see Davison et al. 2005).

98 In a recent study (Hosono et al. 2010), a 'right-handed predator' hypothesis was
99 proposed to explain the effects of pleiotropy on the single-gene speciation of snails. The
100 authors concluded that a gene controlling coiling direction of snails could pleiotropically
101 affects interchiral mating difficulty and anti-predator adaptation because of the 'handedness'
102 of the predator. Because most snails are dextral ('right-handed') (Vermeij 1975), predators
103 tend to be 'right-handed' (have evolved to specialize in the abundant dextral type of snail).
104 Such predators include box crabs (Shoup 1968; Ng and Tan 1985; Dietl and Hendricks 2006),
105 water-scavenger beetle larvae (Inoda et al. 2003), and snail-eating snakes (Hosono et al. 2007;
106 Hosono et al. 2010). Behavioral experiments revealed that right-handed predators tend to fail in
107 attempts to eat sinistral snails because of the left-right asymmetry of their feeding apparatuses

108 and behaviors (Inoda et al. 2003; Dietl and Hendricks 2006; Hosono et al. 2007). Therefore,
109 although a mating disadvantage still exists, sinistral snails will have a survival advantage
110 under right-handed predation. This can potentially promote the fixation of a sinistral allele,
111 and indeed Hosono et al. (2010) found a positive correlation between the distribution of a
112 right-handed predator (snake) and proportion of sinistral lineages in Southeast Asia. Although
113 Hosono et al. (2010) showed a correlation *pattern*, the fixation *process* of the mutant allele in
114 the speciation gene with pleiotropic effects underlying such pattern has not been fully
115 investigated.

116 Here, we theoretically investigate the fixation process of a mutant allele in the
117 speciation gene in single-gene speciation with and without pleiotropic effects. We seek to
118 answer the following questions. (1) How do allele dominance, population size, and delayed
119 inheritance affect single-gene speciation? What kind of mutant allele dominance (e.g.,
120 dominant, recessive, or subdominant) has the highest fixation probability? How do population
121 size and delayed inheritance affect this tendency? (2) How does pleiotropy affect the process
122 of single-gene speciation? On the one hand, when the mutant frequency is low, it would be
123 better for heterozygotes to have the resident phenotype to mate with common resident
124 genotypes because of positive frequency-dependent selection. On the other hand, the mutant

125 phenotype is advantageous under strong viability selection. Because of the conflicting factors
126 acting on heterozygotes, the overall effects of allele dominance and delayed inheritance can
127 be changed by the relative strengths of the pleiotropic effects of the speciation gene.

128

129 **MODEL**

130 To examine the questions of single-gene speciation described above, we consider a general
131 allopatric speciation model. When a panmictic population splits into two geographically
132 divided subpopulations, it is sufficient to compare fixation probabilities of a mutant allele in a
133 single subpopulation to understand the likelihood of speciation (Orr 1991). We construct
134 Wright-Fisher models of haploid or diploid individuals without delayed inheritance and
135 diploid individuals with delayed inheritance to study the mutant allele frequency change
136 through generations with reproductive isolation and viability selection.

137 We assume that mating partners are randomly chosen from the population and that
138 mating between different phenotypes fails with probability r (Table 1) because of either pre-
139 or post-zygotic factors (Slatkin 1982). A common phenotype enjoys an advantage over a rare
140 one because a randomly chosen mate is more likely to be compatible (i.e., the same
141 phenotype). This leads to positive frequency-dependent selection (favoring the more common

142 phenotype) in the mating character.

143

144 **Haploid model**

145 We first consider the simplest case of haploid inheritance. We denote the frequency

146 of the mutant allele (A) by p and that of the wild type allele (a) by $1 - p$. The frequency after

147 mating, \tilde{p} , is

148

$$149 \quad \tilde{p} = \frac{p^2 + (1-r)p(1-p)}{1-2rp(1-p)}, \quad (1)$$

150

151 where r measures the intensity of reproductive isolation between the mutant and wild type (0

152 $\leq r \leq 1$, Table 1). Reproductive isolation is complete if $r = 1$, the mating is random if $r = 0$,

153 and reproductive isolation is partial if $0 < r < 1$. The mutant frequency after one generation,

154 p' , is given by

155

$$156 \quad p' = \frac{(1+s)\tilde{p}}{(1+s)\tilde{p} + 1 \cdot (1-\tilde{p})}, \quad (2)$$

157

158 where s is a positive viability selection coefficient for a mutant (i.e., a mutant has higher

159 survivorship than a wild type). For example, if a mutant snail is sinistral, s represents the
160 relative survival advantage of sinistral snails because of the right-handed predation by snakes
161 (Hoso et al. 2010).

162

163 **Diploid model without delayed inheritance**

164 For the diploid model without delayed inheritance, a mutant arises as a single
165 heterozygote (Aa) in a population of the wild type homozygotes (aa). We denote the degree of
166 dominance of allele A by h such that $h = 0$ and $h = 1$ correspond to completely recessive and
167 dominant mutant alleles, respectively. Under partial dominance ($0 < h < 1$), we consider two
168 models. First, a three-phenotype model in which heterozygotes have an intermediate
169 phenotype of the homozygous phenotypes, and the intensities of reproductive isolation and
170 viability selection are determined by the degree of dominance (h), although this does not
171 apply to snails (Table 1). Second, a two-phenotype (A and a) model in which a heterozygote
172 has phenotypes A and a with probabilities h and $1 - h$, respectively (Appendix S8). We adopt
173 the former model in the main text, but both models give qualitatively similar results (see
174 Discussion). The frequencies of genotypes AA ($= x$) and Aa ($= y$) after mating, \tilde{x} and \tilde{y} , are
175 given by

176

$$\begin{aligned} T\tilde{x} &= x^2 + [1 - (1-h)r]xy + \frac{y^2}{4}, \\ T\tilde{y} &= [1 - (1-h)r]xy + 2(1-r)xz + \frac{y^2}{2} + (1-hr)yz, \end{aligned} \quad (3)$$

178

179 where $T = 1 - 2r[(1-h)xy + xz + hyz]$ and $z (= 1 - x - y)$ represents the frequency of the

180 resident allele homozygote, aa (Table 1). The frequencies in the next generation, x' and y' ,

181 are

182

$$\begin{aligned} x' &= \frac{(1+s)\tilde{x}}{(1+s)\tilde{x} + (1+hs)\tilde{y} + 1 \cdot \tilde{z}}, \\ y' &= \frac{(1+hs)\tilde{y}}{(1+s)\tilde{x} + (1+hs)\tilde{y} + 1 \cdot \tilde{z}}, \end{aligned} \quad (4)$$

184

185 where s is the selective advantage of the mutant phenotype in terms of viability. By definition,

$$186 \quad \tilde{z} = 1 - \tilde{x} - \tilde{y}.$$

187 The condition for the invasion of the mutant allele in a population of infinite size is

188 analyzed by examining the local stability of equilibrium without the mutant ($x = y = 0$) in

189 equation (4). The fixation probability of a mutant for the case with random genetic drift

190 because of a finite population size is examined in three ways. First, assuming r and s values

191 are small, a two-dimensional representation of genotype dynamics (4) can be approximated
192 with one-dimensional dynamics along Hardy-Weinberg equilibrium (Fig. 2). Then applying
193 the diffusion approximation (Crow and Kimura 1970) leads to an analytical formula for the
194 fixation probability with an arbitrary degree of dominance for the mutant allele. Second, for a
195 very small population, because the diffusion approximation is not applicable, the exact
196 fixation probability is numerically calculated with a Markov chain approach (first-step
197 analysis, Pinsky and Karlin 2010). Third, the fixation probability is estimated from extensive
198 Monte Carlo simulations of full dynamics (4) under random genetic drift. We assume
199 symmetric mutation rates for the dominant and recessive alleles and compare their fixation
200 probabilities to predict the allele dominance of sinistral alleles in snails.

201

202 **Diploid model with delayed inheritance**

203 With delayed inheritance, the phenotype of an individual is determined by its
204 mother's genotype. In this model, 6 pairs of genotype-phenotype combination are possible;
205 however, with complete recessiveness or dominance, only 5 pairs can be realized. Here, we
206 assume that the mutant allele A is completely dominant. The counterpart case for a completely
207 recessive mutant can be analyzed in a parallel manner (see Appendix S2). With three

208 genotypes (AA, Aa, and aa) and two phenotypes (A and a), the six genotype-phenotype
 209 combinations are denoted as AA_A, AA_a, Aa_A, Aa_a, aa_A, and aa_a. For example, Aa_A represents
 210 an individual with genotype Aa and phenotype A. Because allele A is dominant, AA_a is simply
 211 impossible in the genetic system of delayed inheritance (Table S1).

212 We assume that the mutation in the speciation gene occurs in the embryo. In the
 213 genetic system of delayed inheritance, the first mutant's phenotype is the same as its wild type
 214 mother. We denote the frequencies of each combination of genotypes and phenotypes, AA_A,
 215 Aa_A, Aa_a, aa_A, and aa_a by x_A , y_A , y_a , z_A , and z_a ($= 1 - x_A - y_a - z_A - z_a$), respectively. Let p ($= x_A$
 216 $+ (y_A + y_a)/2$) and q ($= 1 - p = (y_A + y_a)/2 + z_A + z_a$) be the frequencies of dominant (A) and
 217 recessive (a) alleles. The frequencies after mating are

218

$$\begin{aligned}
 T\bar{x}_A &= p^2 - ry_a \left(x_A + \frac{y_A}{2} \right), \\
 T\bar{y}_A &= p(1 - x_A) - r \left[z_a \left(x_A + \frac{y_A}{2} \right) + y_a \left(x_A + y_A + \frac{z_A}{2} \right) \right], \\
 T\bar{y}_a &= p(1 + x_A - 2p) - r \left[z_a \left(x_A + \frac{y_A}{2} \right) + \frac{y_a z_A}{2} \right], \\
 T\bar{z}_A &= (p - x_A)(1 - p) - \frac{r}{2} [y_A(y_a + z_a) + y_a z_A],
 \end{aligned}
 \tag{5}$$

219

220

221 where $T = 1 - 2r(x_A + y_A + z_A)(y_a + z_a)$. Because phenotype A is favored under viability
 222 selection, the frequencies after viability selection are given by

223

$$224 \quad x'_A = \frac{(1+s)\tilde{x}_A}{W}, y'_A = \frac{(1+s)\tilde{y}_A}{W}, y'_a = \frac{\tilde{y}_a}{W}, z'_A = \frac{(1+s)\tilde{z}_A}{W}, z'_a = \frac{\tilde{z}_a}{W}, \quad (6)$$

225

226 where $W = 1 + s(\tilde{x}_A + \tilde{y}_A + \tilde{z}_A)$ is the mean fitness of the population. See Appendix S2 for the

227 case of a recessive mutant allele.

228

229 Similar to the without-delayed-inheritance model, the condition in which the mutant

230 invades a population of infinite size is analyzed by examining the local stability of

231 mutant-free equilibrium, $x_A = y_A = y_a = z_A = 0$, with 4-dimensional genotype dynamics

232 (5)-(6). For the fixation probability of the mutant in a finite population, genotype dynamics

233 are reduced to a single dimension by assuming small r and s , through Hardy-Weinberg and

234 quasi-equilibrium of genotype-phenotype combination frequencies with the maternal

235 inheritance dynamics, which also leads to an analytical formulation. The first-step analysis for

236 a very small population and the Monte Carlo simulations are performed in the same manner

237 as in the case without delayed inheritance.

238 First-step analysis can also be applied to large populations, but the calculation is

239 formidable when N is large (especially for the diploid model with delayed inheritance that has

240 results to the $N = 10$, $N = 1,000$ (Monte Carlo simulations), and $N \rightarrow \infty$ (diffusion
241 approximation) conditions.

242

243 **RESULTS**

244 Through a deterministic analysis of infinite populations, we confirm that if the
245 degree of reproductive isolation between mating phenotypes is larger than the coefficient of
246 viability selection ($r > s$), the system shows bistability: the monomorphism of either allele (A
247 or a) is stably maintained under positive frequency-dependent selection due to reproductive
248 isolation for haploid and diploid conditions as well as delayed and non-delayed inheritance
249 conditions. A rare mutant allele cannot invade infinite populations as predicted by the classic
250 theory (Bateson 1909; Dobzhansky 1936; Muller 1942). Thus, genetic drift in finite
251 populations is a prerequisite for single-gene speciation with weak viability selection ($r > s$)
252 (Gavrilets 2004).

253

254 **Invasion conditions in deterministic models**

255 We demonstrate that pleiotropic effects can promote single-gene speciation, as
256 proposed by Hosoi et al. (2010). Because a single speciation gene causes positive

257 frequency-dependent selection, viability selection must be strong enough for the mutant allele
258 to successfully invade a population (Fig. 3). The required selection coefficient for a mutant
259 allele to invade is $s > r/(1-r)$ in haploid and diploid models with complete dominance (i.e.,
260 the mutant is either completely dominant or recessive) and $s > r/(1-hr)$ for the diploid
261 model with partial dominance (Appendix S1, S2, and S8). In the haploid model, equations (1)
262 and (2) are approximated as $p' \approx (1+s)(1-r)p$ if the mutant frequency is small ($p \approx 0$).
263 When $(1+s)(1-r) < 1$, the system is bistable and positive frequency-dependent selection
264 excludes rare alleles. There are two locally stable equilibria at $p = 0$ and $p = 1$, and a locally
265 unstable equilibrium, $p_c = [r(1+s) - s] / [r(2+s)]$, that divides two basins of attraction. As
266 the mutant allele becomes more selectively favored ($s (> 0)$ is increased), the unstable
267 equilibrium moves closer to zero and eventually disappears once s is large enough to satisfy
268 $(1+s)(1-r) = 1$. When $(1+s)(1-r) > 1$ or $s > r/(1-r)$, there is a globally stable equilibrium
269 at $p = 1$ and the mutant allele increases and eventually fixes irrespective of its initial
270 frequency (Fig. 3). Note that invasion is impossible when reproductive isolation is complete
271 ($r = 1$), and this again suggests the importance of genetic drift in small populations.

272 For the diploid model, partial dominance makes single-gene speciation more
273 feasible because heterozygotes can simultaneously maintain their mating probability and

274 survival advantage. We derive the condition for the mutant allele to be able to invade the wild
275 type population as $s > r/(1 - hr)$ when $h \neq 0$ by analyzing recursion equations (3) and (4)
276 (Appendix S1). Interestingly, the invasion condition of the complete recessive ($h = 0$) allele (s
277 $> r/(1 - r)$) differs from $s > r$, that is the limit of $h \rightarrow 0$ for the invasion condition of the
278 partially dominant mutant (Appendix S1) because with small h in the partial dominance
279 model, there is a stable internal (coexisting) equilibrium, which does not exist for complete
280 recessiveness (Fig. S4). Heterozygotes with a completely recessive mutant allele are neutral
281 for viability selection, but the invasion condition is equivalent to the completely dominant (h
282 $= 1$) allele (Fig. 3). In addition, because of a locally stable equilibrium in which the mutant
283 allele coexists with the resident allele if r is large and h is small (Fig. S4), the invasibility of a
284 mutant (Fig. 3) does not necessarily imply its fixation in the population. For the diploid model
285 with delayed inheritance, the invasion condition in infinite populations is $(1 + s)(1 - r) > 1$
286 (Appendix S2), which is identical to the haploid and diploid models without delayed
287 inheritance (Fig. 3). However, the largest eigenvalue of the Jacobian matrix in the linearized
288 system is smaller than the dominant allele in the diploid model without delayed inheritance
289 (Appendix S2), which corresponds to the fact that delayed inheritance makes the invasion of a
290 mutant more feasible in a finite population, which we discuss later. Note that under positive

291 frequency-dependent selection, viability selection does not need to be constantly strong. Once
292 the mutant allele frequency exceeds the unstable equilibrium, the mutant phenotype becomes
293 advantageous in mating and strong viability selection is no longer necessary.

294

295 **Fixation in a finite population with haploid inheritance**

296 The change in allele frequency after one generation, $\Delta p = p' - p$, in the haploid
297 model is

298

$$299 \quad \Delta p = \frac{p(1-p)[r(2p-1)+s-sr(1-p)]}{(1+s\tilde{p})[1-2rp(1-p)]}, \quad (7)$$

300

301 which is derived from equations (1) and (2). Assuming r and s are small, we can consider a
302 continuous time model for the change in allele frequency. Neglecting higher order terms for r
303 and s , we have the deterministic dynamics,

304

$$305 \quad \dot{p} = p(1-p)[r(2p-1)+s]. \quad (8)$$

306

307 Equation (8) has two stable equilibria at $p = 0$ and $p = 1$, and an internal unstable equilibrium

308 at $p = p_c = (1 - s/r)/2$ when $r > s$. However, if $s \geq r$, only $p = 1$ is locally stable. When s
 309 $= 0$, the unstable equilibrium is at $p = 1/2$ and the derivative of allele frequency dynamics is
 310 negative when p is smaller than $1/2$ and positive when p is larger than $1/2$ (solid gray line in
 311 Fig. 4A). This result for the haploid model serves as the baseline when we discuss the effects
 312 of dominance and delayed inheritance.

313 If the population is finite, a single mutant can go to fixation and replace the wild
 314 type even when $r > s$. Assuming r and s are small and the population size (N) is large, we
 315 obtain the fixation probability of a single mutant by applying the diffusion approximation as

$$317 \quad \rho = u(1/N) = \frac{1/N}{\int_0^1 \exp\left[\frac{R}{2}(p - p^2) - \frac{S}{2}p\right] dp}, \quad (9)$$

318
 319 where $R = 4Nr$ and $S = 4Ns$. If and only if the locally unstable equilibrium is less than $1/3$,
 320 $p_c = (1 - S/R)/2 < 1/3$, there exists some N with which the fixation probability ρ is higher
 321 than that of a neutral mutant ($1/N$) (one-third law, Nowak et al. 2004).

322

323 **Fixation in a finite population with diploid inheritance**

324 *The one-dimensional diffusion process along the curve of Hardy-Weinberg equilibrium*

325 The dynamics of dominant and recessive alleles in the diploid models are also
326 subject to positive frequency-dependent selection, but variation in the position of the internal
327 equilibrium and selection gradient along the mutant allele frequency depends heavily on
328 which allele is dominant, which has a large effect on the process of fixation. Namely, a
329 dominant allele is favored over a recessive allele at intermediate frequencies; whereas, a
330 recessive allele is favored when it is at either low or high frequencies (compare red and blue
331 dashed curves in Fig. 4D). To show this and to evaluate the fixation probability of a mutant
332 later, we approximate the two-dimensional genotype frequency dynamics of the diploid model
333 to one-dimensional allele frequency dynamics. Genotype frequency dynamics are not strictly
334 at Hardy-Weinberg (HW) equilibrium, and this deviation is caused by reproductive isolation
335 and viability selection (Fig. 2). However, we show that if both r and s are small, frequency
336 dynamics first approach HW equilibrium and slowly converge to a locally stable equilibrium
337 at $p = 0$ or 1 (Crow and Kimura 1970 demonstrated this without viability selection).
338 Assuming that r and s are in the order of ε , which is a small positive constant, we expand the
339 dynamics of equations (3) and (4) in Taylor series with respect to ε . The leading order
340 dynamics for the zygote frequencies becomes

341

$$\begin{aligned} 342 \quad x' &= p^2 + O(\varepsilon), \\ y' &= 2p(1-p) + O(\varepsilon). \end{aligned} \tag{10}$$

343

344 Thus, up to the leading order, genotype frequencies are in HW equilibrium. From this, it

345 follows that the allele frequencies do not change with time ($p' = p$) up to the leading order.

346 By assuming a large population size, small values of r and s , and HW equilibrium (10), we

347 can approximate the deterministic allele frequency dynamics by

348

$$349 \quad \dot{p} = p(1-p) \left\{ r \left[p(2p^2 - 1) - h(6p^2 - 6p + 1) \right] + s \left[p + h(1 - 2p) \right] \right\}. \tag{11}$$

350

351 The scaled derivatives of the frequency dynamics when $h = 0, 1/2,$ and 1 without viability

352 selection ($s = 0$) are shown by dotted lines (Figs. 4 and S1).

353

354 *Effect of dominance on the fixation probability of a mutant in a large finite population*

355 Despite the large difference in the frequency-dependent fitness profiles between

356 dominant and recessive alleles (Fig 4D), both alleles have the same fixation probability if

357 there is no viability selection in large populations (Fig. 5H). From the allele frequency

358 dynamics (11) under Hardy-Weinberg equilibrium that is approximately followed throughout
 359 the process for small r and s , we obtain the fixation probability of a single mutant allele,
 360 $\rho_h = u(1/(2N))$, with the diffusion approximation (Appendix S3) where $u(p)$ is the fixation
 361 probability of a mutant with the initial frequency p . The fixation probability of a single mutant
 362 ρ_h for a given degree h of dominance is given by

$$364 \quad \rho_h = \frac{1/(2N)}{\int_0^1 \exp \left\{ Ry(1-y) \left[\frac{y}{2}(1+y) - h(2y-1) \right] - Sy \left[\frac{y}{2} + h(1-y) \right] \right\} dy}, \quad (12)$$

365
 366 where $R = 4Nr$ and $S = 4Ns$, as defined before. Thus, the recessive ($h = 0$) and dominant ($h =$
 367 1) mutants have exactly the same fixation probability if there is no viability selection ($s = 0$),

$$369 \quad \rho_0 = \frac{1/(2N)}{\int_0^1 \exp \left[\frac{R}{2}(1-y)y^2(1+y) \right] dy} = \frac{1/(2N)}{\int_0^1 \exp \left[\frac{R}{2}y(1-y)^2(2-y) \right] dy} = \rho_1, \quad (13)$$

370
 371 which can be shown by changing the variables in the integral (Appendix S3).

372

373 *Very small populations*

374 When population size is very small and viability selection is absent, the recessive
375 mutant allele has a higher fixation probability than the dominant allele. We show this result
376 with Monte Carlo simulations (Fig. 5E) and numerical calculations of exact fixation
377 probabilities using first-step analysis (Fig. 5B, Appendix S5, S6). The discrepancy between
378 the cases of large (diffusion approximation results) and small population sizes could be
379 because of the different contributions of absolute numbers of individuals to the frequency
380 dynamics. Although we assume that a mutant first arises as a single heterozygous individual
381 in the diploid model, the initial mutant frequency is higher in a small population. Thus, the
382 first heterozygous individual with a dominant mutant allele is more strongly selected against
383 than a recessive mutant allele in small populations (Fig. 4D).

384

385 *Effect of delayed inheritance*

386 As shown in equations (14) and (15) below, delayed inheritance halves the strength
387 of positive frequency-dependent selection (Fig. 4), which increases the fixation probability of
388 a mutant in large populations (Fig. 5I). Assuming HW equilibrium when r and s are small
389 (Appendix S4), the approximated frequency dynamics of the dominant mutant allele in the
390 diploid model with delayed inheritance is given by

391

392
$$\dot{p} = \frac{1}{2} p(1-p)^2 [-r(2p^2 - 4p + 1) + s]. \quad (14)$$

393

394 Furthermore, the frequency dynamics of the recessive mutant allele is

395

396
$$\dot{p} = \frac{1}{2} p^2(1-p) [r(2p^2 - 1) + s]. \quad (15)$$

397

398 Comparing these equations to equation (11) with $h = 1$ and $h = 0$, we find that the right-hand

399 side of equations (14) and (15) are exactly one-half of the right-hand side of equation (11)

400 with $h = 1$ and $h = 0$, respectively (solid lines in Fig. 4). Therefore, regardless of whether the

401 mutant allele is dominant or recessive, the fixation probabilities for a mutant are higher when

402 delayed inheritance is present than when delayed inheritance is absent (Fig. 5I, Appendix S4).

403 The fact that the magnitudes of r and s relative to the strength of genetic drift $1/N$ are halved

404 may be reinterpreted to mean that delayed inheritance effectively halves the effective

405 population size. This is probably because the phenotype is determined only by the mother's

406 genotype with no contribution from the father. The tendency for the model with delayed

407 inheritance to have higher fixation probabilities remains the same in small populations where

408 diffusion approximation cannot apply (Figs. 5C, 5F, Appendix S7). With delayed inheritance,
409 fixation probabilities can be increasing functions of reproductive isolation (r) when viability
410 selection is strong ($s \gg 1$) and the population size is very small ($N = 3$), which contrasts the
411 general tendency (i.e., for fixation probabilities to be decreasing functions of reproductive
412 isolation) (Fig. S6).

413

414 *Effect of reproductive isolation and viability selection*

415 Positive frequency-dependent selection and viability selection work on the mutant
416 phenotype; therefore, individuals with the mutant phenotype get conflicting effects from the
417 two selection pressures when the mutant allele frequency is low. When reproductive isolation
418 is relatively weak, the survival advantage of the mutant phenotype exceeds its mating
419 disadvantage; on the other hand, with relatively strong reproductive isolation, the survival
420 advantage of the mutant phenotype cannot compensate for its mating disadvantage when the
421 mutant is rare. In large populations, the dominant and recessive mutant alleles have the same
422 fixation probability without pleiotropy (when $s = 0$: Fig. 5), whereas the dominant mutant
423 allele has higher fixation probability when $r = 0$ (Haldane's sieve: see Discussion). Thus
424 fixation probabilities of the dominant mutant allele are always higher than those of the

425 recessive allele. Delayed inheritance halves selection pressures (equations 14 and 15); this is
426 advantageous when positive frequency-dependent selection due to reproductive isolation is
427 strong (Fig. 4), but is not advantageous when viability selection is strong. Therefore, the
428 dominant mutant allele without delayed inheritance has the highest fixation probability when
429 reproductive isolation (Nr) is weak and viability selection (Ns) is strong, whereas the
430 dominant mutant allele with delayed inheritance has the highest fixation probability when
431 reproductive isolation is strong and viability selection is weak in large populations (Fig. 6C).
432 In small populations, the recessive mutant allele with delayed inheritance has the highest
433 fixation probability when reproductive isolation is strong and viability selection is weak (Figs.
434 6A, 6B). Therefore, the more frequently fixed allele can be dominant when viability selection
435 is relatively strong (Fig. 6), which is in contrast to speciation without pleiotropy.

436

437 **DISCUSSION**

438 In finite populations without pleiotropy, dominant and recessive alleles have the
439 same fixation probability in large populations; however, a recessive allele has a higher
440 fixation probability in very small populations. The effects of population size are contrasting,
441 but most left-right reversals are likely to have occurred in small isolated populations (Orr

442 1991; Hosoi 2012). Therefore, the recessive mutant allele will fix more frequently than the
443 dominant allele in the absence of right-handed predation, if the dominant and recessive
444 mutations arise in the same probability.

445 There are conflicting arguments about allele dominance; Orr (1991) wrote “the
446 probability of fixation of a maternal mutation is roughly independent of its dominance” in
447 dioecious populations, whereas hermaphroditic populations with selfing “...*decrease* the
448 chance that a dominant mutation will be fixed.” In contrast, van Batenburg and Gittenberger
449 (1996) showed that the dominant mutant allele has a higher fixation probability. We point out
450 that this discrepancy is mainly because of different assumptions of the initial numbers of the
451 mutant allele. Both Orr (1991) and we computed the fixation probability of a single mutant,
452 whereas van Batenburg and Gittenberger (1996) even considered 16 invaders with the total
453 population size 32, assuming mass invasion from neighboring sinistral populations. By
454 accounting for the assumptions of each argument, the conflicting results can be explained
455 because the recessive mutant allele has a higher fitness when it is rare, whereas the dominant
456 mutant allele has a higher derivative when the frequency is intermediate (Fig. 4D). We
457 changed the initial numbers of mutants in Monte Carlo simulations and obtained results to
458 support this claim (data not shown). The fixation probability is usually calculated for a single

459 *de novo* mutation. Thus, as long as the initial mutant is a single heterozygote, we analytically
460 and numerically showed that the recessive mutant allele has a higher fixation probability in
461 small populations and both alleles have the same probability in large populations (Fig. 5).

462 The effect of reproductive isolation and viability selection (Fig. 6) is consistent with
463 “Haldane’s sieve”, where there is a bias against the establishment of recessive adaptive alleles
464 (Haldane 1924, 1927; Turner 1981). Previous studies revealed that certain factors, including
465 self-fertilization (Charlesworth 1992), adaptation from standing genetic variation (Orr and
466 Betancourt 2001), and spatial structure (Whitlock 2003), can change the fixation bias of allele
467 dominance. Our results showed that the adaptive mutation that pleiotropically contributes to
468 reproductive isolation can also change this bias.

469 We consider two cases of partial dominance ($h = 0.5$) in the diploid model without
470 delayed inheritance. Although these do not apply to snails, the results would be important for
471 understanding general single-gene speciation processes. Because of different fitness gradients
472 along allele frequencies (Fig. S1), the three-phenotype model has a higher fixation probability
473 than the two-phenotype model, which has similar results as the haploid model (Figs. 5B, 5E,
474 5H, S2, and S3). With pleiotropy, the fixation probability in the three-phenotype model is the
475 highest when reproductive isolation is strong and viability selection is weak in large

476 populations (Fig. S5C), while it is the highest in intermediate intensity of reproductive
477 isolation and viability selection in small populations (Figs. S5A and S5B).

478 In single-gene speciation in snails, the intensity of interchiral mating difficulty, r ,
479 should be an important parameter; interchiral mating is almost impossible in flat-shelled
480 snails that perform two-way face-to-face copulation (large r), whereas it is relatively easy for
481 tall-shelled snails that can copulate by shell mounting (small r) (Asami et al. 1998). Therefore,
482 even with the same population size and right-handed predation pressure, the frequently fixed
483 allele dominance can be changed (Fig. 6A). When right-handed predation is weak or absent
484 and interchiral mating is difficult (flat-shelled snails), the frequently fixed allele should be
485 recessive. On the other hand, the frequently fixed allele can be dominant when right-handed
486 predation is strong and interchiral mating is easy (tall-shelled snails).

487 We have calculated fixation probabilities for various values of N , r , s , and the
488 dominance of the mutant allele. Phylogenetic information (Ueshima and Asami 2003; Hosoi et
489 al. 2010) can be used to infer these parameters because the number of left-right reversals in
490 the phylogeny is influenced by fixation probabilities. Let P_S be the duration that the snail
491 phenotype remains sinistral, and P_D be the duration for dextrality. The expected sojourn time
492 in the sinistral phenotype is $P_S = 1/(N\mu\rho_D)$, where μ is the mutation rate of the speciation gene

493 changing to the dextral allele and ρ_D is the fixation probability of the mutant dextral allele.
494 Assuming that the mutation is symmetrical and population size is constant, the ratio of these
495 values is given by $P_S/P_D = (N\mu\rho_D)/(N\mu\rho_S) = \rho_D/\rho_S$. If left-right reversals have occurred
496 frequently, the ratio estimated from the phylogeny data should approach the theoretical
497 prediction. The extent of assortative mating, r , (Asami et al. 1998) and biased predation
498 pressure by right-handed predators, s , (Hoso et al. 2007; Hoso et al. 2010) are known from
499 experiments. Thus, it would be possible to estimate the population size and allele dominance
500 by statistical inference. However, in addition to the somewhat arbitrary assumptions of
501 constant population size, symmetrical mutation, and equilibrium states, reconstruction of
502 ancestral states is generally challenging when the trait evolves adaptively (Cunningham 1999).
503 Furthermore, we did not consider gene flow between spatially neighboring dextral and
504 sinistral populations (Davison et al. 2005) or internal selection against left-right reversal
505 (Utsuno et al. 2011). Thus, we propose these estimations as a future research subject.

506 In conclusion, although the conventional theory by Bateson, Dobzhansky and
507 Muller is still valid, our study has shown that single-gene speciation is likely to be more
508 realizable than previous studies have assumed by combining various factors including
509 recessiveness, delayed inheritance, small population size, and pleiotropic effects that increase

510 mutant viability. Specifically, delayed inheritance and pleiotropic effects of the speciation
511 gene (e.g., right-handed predation on snails) can promote single-gene speciation, which
512 supports the hypothesis that right-handed predation by specialist snakes is responsible for
513 frequent left-right reversals of land snails in Southeast Asia (Hoso et al. 2010). Sinistral
514 species have frequently evolved outside the snake range without right-handed predation, and
515 in this case, our study suggests that allele dominance is important as well as small population
516 size and delayed inheritance (Orr 1991). Interestingly, population size and pleiotropy can
517 change the effects of allele dominance and delayed inheritance on speciation. Ueshima and
518 Asami (2003) constructed a molecular phylogeny and speculated that the dextral allele
519 appears to be dominant for *Euhadra* snails based on the breeding experiments with a
520 *Bradybaena* species, citing van Batenburg and Gittenberger (1996); however, caution is
521 needed because reversal could occur by a *de novo* mutation and viability selection by
522 right-handed predators might be involved in speciation (Hoso et al. 2010). Recent
523 technological developments in molecular biology make it possible to investigate the
524 dominance of alleles in ecologically important traits as well as their ecological and
525 evolutionary effects (e.g., Rosenblum et al. 2010). Although the search for a coiling gene (the
526 speciation gene) in snails is still underway (e.g., Grande and Patel 2009; Kuroda et al. 2009),

527 our prediction—that the recessive allele has a higher fixation probability in the absence of
528 specialist predators ($s = 0$) for flat-shelled snails (large r), whereas the dominant allele can
529 have a higher fixation probability in the presence of specialist predators ($s > 0$) for tall-shelled
530 snails (small r)—will be testable. This hypothesis could be tested, for example, by analyzing
531 the correlations between the presence of right-handed predators and sinistral allele
532 dominance.

533

534 **ACKNOWLEDGEMENTS**

535 We thank Dr. Masaki Hosoi for discussion and valuable comments on our earlier manuscript.
536 We also thank two anonymous reviewers, Prof. Stephen P. Ellner, Prof. Hisashi Ohtsuki, Whit
537 Hairston, Joseph L. Simonis, and members of the Sasaki-Ohtsuki lab, the Hairston lab, and
538 the Ellner lab for their helpful comments. M. Y. was supported by a Research Fellowship of
539 the Japan Society for the Promotion of Science (JSPS) for Young Scientist (21-7611) and is
540 supported by JSPS Postdoctoral Fellowship for Research Abroad (24-869). A. S. is supported
541 by MEXT/JSPS KAKENHI, and the Graduate University for Advanced Studies (Sokendai).

542

543 **LITERATURE CITED**

544 Arnaud, J. F., and G. Laval. 2004. Stability of genetic structure and effective population size

545 inferred from temporal changes of microsatellite DNA polymorphisms in the land
546 snail *Helix aspersa* (Gastropoda: Helicidae). *Biological Journal of the Linnean Society*
547 82:89-102.

548 Asami, T., R. H. Cowie, and K. Ohbayashi. 1998. Evolution of mirror images by sexually
549 asymmetric mating behavior in hermaphroditic snails. *American Naturalist*
550 152:225-236.

551 Bank, C., R. Bürger, and J. Hermisson. 2012. The limits to parapatric speciation:
552 Dobzhansky-Muller incompatibilities in a continent-island model. *Genetics*
553 191:845-863.

554 Bateson, W. 1909. Heredity and variation in modern lights. Pp. 85-101 in A. C. Seward, ed.
555 *Darwin and Modern Science*. Cambridge University Press, Cambridge.

556 Boycott, A. E., C. Diver, S. L. Garstang, and F. M. Turner. 1930. The inheritance of
557 sinistrality in *Limnaea peregra* (Mollusca, Pulmonata). *Philosophical Transactions of*
558 *the Royal Society B* 219:51-131.

559 Charlesworth, B. 1992. Evolutionary rates in partially self-fertilizing species. *American*
560 *Naturalist* 140:126-148.

561 Coyne, J. A., and H. A. Orr. 2004. *Speciation*. Sinauer Associates, Inc., Sunderland.

562 Crow, J. F., and M. Kimura. 1970. *An Introduction to Population Genetics Theory*. Harper &
563 Row, Publishers, Inc., New York.

564 Cunningham, C. W. 1999. Some limitations of ancestral character-state reconstruction when
565 testing evolutionary hypotheses. *Syst. Biol.* 48:665-674.

566 Davison, A., S. Chiba, N. H. Barton, and B. Clarke. 2005. Speciation and gene flow between
567 snails of opposite chirality. *PLoS Biology* 3:e282.

568 Degner, E. 1952. Der erbgang der inversion bei *Laciniaria biplicata* MTG. *Mitteilungen der*
569 *Hamburg Zoologisches Museum und Institut* 51:3-61.

570 Dietl, G. P., and J. R. Hendricks. 2006. Crab scars reveal survival advantage of left-handed
571 snails. *Biology Letters* 2:439-442.

572 Dobzhansky, T. 1936. Studies on hybrid sterility. II. Localization of sterility factors in
573 *Drosophila pseudoobscura* hybrids. *Genetics* 21:113-135.

574 Felsenstein, J. 1981. Skepticism towards Santa Rosalia, or why are there so few kinds of
575 animals? *Evolution* 35:124-138.

576 Freeman, G., and J. W. Lundelius. 1982. The developmental genetics of dextrality and
577 sinistrality in the gastropod *Lymnaea peregra*. *Wilhelm Roux's Archives of*
578 *Developmental Biology* 191:69-83.

579 Gavrillets, S. 2004. *Fitness Landscapes and the Origin of Species*. Princeton University Press,

580 Princeton.

581 Gittenberger, E. 1988. Sympatric speciation in snails: a largely neglected model. *Evolution*
582 42:826-828.

583 Gittenberger, E., T. D. Hamann, and T. Asami. 2012. Chiral speciation in terrestrial pulmonate
584 snails. *PLoS ONE* 7:e34005.

585 Grande, C., and N. H. Patel. 2009. Nodal signalling is involved in left-right asymmetry in
586 snails. *Nature* 457:1007-1011.

587 Haldane, J. B. S. 1924. A mathematical theory of natural and artificial selection, Part I.
588 *Transactions of the Cambridge Philosophical Society* 23:19-41.

589 Haldane, J. B. S. 1927. A mathematical theory of natural and artificial selection, Part V:
590 selection and mutation. *Proc. Camb. Philos. Soc.* 28:838-844.

591 Hosoi, M. 2012. Non-adaptive speciation of snails by left-right reversal is facilitated on
592 oceanic islands. *Contributions to Zoology* 81:79-85.

593 Hosoi, M., T. Asami, and M. Hori. 2007. Right-handed snakes: convergent evolution of
594 asymmetry for functional specialization. *Biology Letters* 3:169-172.

595 Hosoi, M., Y. Kameda, S. P. Wu, T. Asami, M. Kato, and M. Hori. 2010. A speciation gene for
596 left-right reversal in snails results in anti-predator adaptation. *Nature Communications*
597 1:133.

598 Inoda, T., Y. Hirata, and S. Kamimura. 2003. Asymmetric mandibles of water-scavenger
599 larvae improve feeding effectiveness on right-handed snails. *American Naturalist*
600 162:811-814.

601 Johnson, M. S. 1982. Polymorphism for direction of coil in *Partula suturalis*: behavioural
602 isolation and positive frequency dependent selection. *Heredity* 49:145-151.

603 Kirkpatrick, M., and V. Ravigné. 2002. Speciation by natural and sexual selection: Models
604 and experiments. *American Naturalist* 159:S22-S35.

605 Kuroda, R., B. Endo, M. Abe, and M. Shimizu. 2009. Chiral blastomere arrangement dictates
606 zygotic left-right asymmetry pathway in snails. *Nature* 462:790-794.

607 Muller, H. J. 1942. Isolating mechanisms, evolution, and temperature. *Biological Symposia*
608 6:71-125.

609 Murray, J., and B. Clarke. 1976. Supergenes in polymorphic land snails II. *Partula suturalis*.
610 *Heredity* 37:271-282.

611 Ng, P. K. L., and L. W. H. Tan. 1985. 'Right handedness' in heterochelous calappoid and
612 xanthoid crabs: suggestion for a functional advantage. *Crustaceana* 49:98-100.

613 Nowak, M. A., A. Sasaki, C. Taylor, and D. Fudenberg. 2004. Emergence of cooperation and
614 evolutionary stability in finite populations. *Nature* 428:646-650.

615 Okumura, T., H. Utsuno, J. Kuroda, E. Gittenberger, T. Asami, and K. Matsuno. 2008. The
616 development and evolution of left-right asymmetry in invertebrates: lessons from
617 *Drosophila* and snails. *Developmental Dynamics* 237:3497-3515.

618 Orr, H. A. 1991. Is single-gene speciation possible? *Evolution* 45:764-769.

619 Orr, H. A. 1996. Dobzhansky, Bateson, and the genetics of speciation. *Genetics*
620 144:1331-1335.

621 Orr, H. A., and A. J. Betancourt. 2001. Haldane's sieve and adaptation from the standing
622 genetic variation. *Genetics* 157:875-884.

623 Pinsky, M. A., and S. Karlin. 2010. *An Introduction to Stochastic Modeling*. Academic Press,
624 Burlington.

625 Rosenblum, E. B., H. Römpler, T. Schöneberg, and H. E. Hoekstra. 2010. Molecular and
626 functional basis of phenotypic convergence in white lizards at White Sands. *Proc. Natl.*
627 *Acad. Sci. U. S. A.* 107:2113-2117.

628 Rundle, H. D., and P. Nosil. 2005. Ecological speciation. *Ecology Letters* 8:336-352.

629 Schilthuizen, M., and A. Davison. 2005. The convoluted evolution of snail chirality.
630 *Naturwissenschaften* 92:504-515.

631 Schluter, D. 2009. Evidence for ecological speciation and its alternative. *Science*
632 323:737-741.

633 Servedio, M. R., G. S. Van Doorn, M. Kopp, A. M. Frame, and P. Nosil. 2011. Magic traits in
634 speciation: 'magic' but not rare? *Trends in Ecology & Evolution* 26:389-397.

635 Shoup, J. B. 1968. Shell opening by crabs of genus *Calappa*. *Science* 160:887-888.

636 Slatkin, M. 1982. Pleiotropy and parapatric speciation. *Evolution* 36:263-270.

637 Stone, J., and M. Björklund. 2002. Delayed prezygotic isolating mechanisms: evolution with
638 a twist. *Proceedings of the Royal Society of London Series B-Biological Sciences*
639 269:861-865.

640 Turner, J. R. G. 1981. Adaptation and evolution in *Heliconius*: A defense of neoDarwinism.
641 *Annu. Rev. Ecol. Syst.* 12:99-121.

642 Ueshima, R., and T. Asami. 2003. Single-gene speciation by left-right reversal - A land-snail
643 species of polyphyletic origin results from chirality constraints on mating. *Nature*
644 425:679.

645 Utsuno, H., T. Asami, T. J. M. Van Dooren, and E. Gittenberger. 2011. Internal selection
646 against the evolution of left-right reversal. *Evolution* 65:2399-2411.

647 van Batenburg, F. H. D., and E. Gittenberger. 1996. Ease of fixation of a change in coiling:
648 Computer experiments on chirality in snails. *Heredity* 76:278-286.

649 Vermeij, G. J. 1975. Evolution and distribution of left-handed and planispiral coiling in snails.

650 Nature 254:419-420.

651 Whitlock, M. C. 2003. Fixation probability and time in subdivided populations. *Genetics*
652 164:767-779.

653

654

655

656 **TABLES**

657 **Table 1.** The diploid model without delayed inheritance ($h = 0$: a is a dominant allele, $h = 1$: A
 658 is a dominant allele)

659

Mating comb.	Mating prob.	AA	Aa	aa
AA × AA	x^2	1	0	0
AA × Aa	$2[1 - (1 - h)r]xy$	1/2	1/2	0
AA × aa	$2(1 - r)xz$	0	1	0
Aa × Aa	y^2	1/4	1/2	1/4
Aa × aa	$2(1 - hr)yz$	0	1/2	1/2
aa × aa	z^2	0	0	1

660

661

662

663 **FIGURE LEGENDS**

664 **Figure 1.** Chirality inheritance determined by maternal effects of dominant dextral (D) and
665 recessive sinistral (s) alleles at a single nuclear locus (delayed inheritance). Black and gray
666 spirals indicate dextral and sinistral phenotypes, respectively. In the second generation,
667 individuals of the same genotype (Ds) develop into the opposite enantiomorph depending on
668 the maternal genotype (DD or ss). Note that snails are androgynous.

669

670 **Figure 2.** Representative example for the trajectory of the fixation process of a mutant allele
671 that starts as a single heterozygote (black line) in the diploid model without delayed
672 inheritance. *X*-axis: frequency of the resident allele homozygotes, *aa* (*z*). *Y*-axis: frequency of
673 the mutant allele homozygotes, *AA* (*x*). Note that $x + z \leq 1$ (dashed line). The initial condition
674 is at $(z, x) = (1 - 1/N, 0)$ (black point). The gray curve $(x = 1 + z - 2\sqrt{z})$ indicates HW
675 equilibrium. Parameter values are $N = 30$, $r = 0.1$, $s = 0.1$, and $h = 1$.

676

677 **Figure 3.** Deterministic invasion conditions for a mutant allele. Invasion is possible above
678 each line. *X*-axis: reproductive isolation parameter (*r*). *Y*-axis: viability selection coefficient
679 (*s*). Completely recessive and dominant mutant alleles ($h = 0$ and 1) require a large selection

680 coefficient for invasion, whereas partially dominant alleles (e.g., $h = 0.5$) require a smaller
681 selection coefficient. Note that the invasion condition of the completely recessive mutant
682 allele differs from the limit of $h \rightarrow 0$ (dotted line).

683

684 **Figure 4.** Allele frequency dynamics affected by positive frequency-dependent selection due
685 to reproductive isolation (indicated by white arrows). Here is no viability selection ($s = 0$).
686 X-axis: mutant allele frequency (p). Y-axis: scaled derivatives of the mutant allele (\dot{p}/r). A:
687 The haploid model (solid gray line, eq. 8). An unstable equilibrium at $p = 1/2$ (white point)
688 divides two basins of attraction. Stable equilibria are at $p = 0$ and 1 (black points). B: The
689 diploid models with the dominant mutant allele without delayed inheritance (dotted red line,
690 eq. 11 when $h = 1$) and with delayed inheritance (solid red line, eq. 14). An unstable
691 equilibrium is at $p = 1 - 1/\sqrt{2}$. C: The diploid models with the recessive mutant allele
692 without delayed inheritance (dotted blue line, eq. 11 when $h = 0$) and with delayed inheritance
693 (solid blue line, eq. 15). An unstable equilibrium is at $p = 1/\sqrt{2}$. D: Comparison of the
694 diploid models with the dominant (red) and recessive (blue) alleles. Intersection points are at
695 $p = 1/2 - \sqrt{3}/6$ and $1/2 + \sqrt{3}/6$ (gray lines).

696

697 **Figure 5.** Relative fixation probabilities of a single mutant with reproductive isolation to that
698 of a neutral mutant. Here is no viability selection ($s = 0$). A-F: X-axis is reproductive isolation
699 parameter (r). G-I: X-axis is four times the product of reproductive isolation parameter and
700 effective population size ($4Nr$). Y-axis is the product of fixation probability and effective
701 population size ($N\rho$ in the haploid model and $2N\rho$ in the diploid models). A-C: $N = 3$
702 (first-step analyses and Monte Carlo simulations), D-F: $N = 10$ (Monte Carlo simulations),
703 G-I: $N \rightarrow \infty$ (diffusion approximation) and $N = 1000$ (Monte Carlo simulations). A, D, G:
704 Solid gray lines: the haploid model. B, C, E, F, H, I: Blue lines: the recessive mutant allele,
705 red lines: the dominant mutant allele, green lines: the partial dominance model with two
706 phenotypes ($h = 0.5$), solid lines: with delayed inheritance, dotted lines: without delayed
707 inheritance. Points represent the results of Monte Carlo simulations. The solid gray line in Fig.
708 5G and the dotted green line in Fig. 5H are identical. The dotted blue and red lines (the
709 diploid model without delayed inheritance) are overlapping in Fig. 5H. The solid blue and red
710 lines (the diploid model with delayed inheritance) are overlapping in Fig. 5I.

711

712 **Figure 6.** The alleles with the highest fixation probabilities given certain strength of
713 reproductive isolation and viability selection. Note that black lines do not represent invasion

714 conditions unlike Fig. 3. A: $N = 3$ (first-step analyses), B: $N = 10$ (Monte Carlo simulations),
715 C: $N \rightarrow \infty$ (diffusion approximation). A, B: X-axis is reproductive isolation parameter (r)
716 and Y-axis is viability selection coefficient (s). C: X-axis is four times the product of
717 reproductive isolation parameter and effective population size ($4Nr$) and Y-axis is four times
718 the product of viability selection coefficient and effective population size ($4Ns$). When $4Ns =$
719 0, both dominant and recessive mutant alleles with delayed inheritance have the same fixation
720 probability (dashed line). DI: delayed inheritance.

1 Online Supporting Information

2 Appendix S1: Invasion condition in the diploid model without delayed inheritance

3 We denote the frequencies of the genotypes, AA, Aa, and aa by x , y , and z ($= 1 - x - y$). The
4 frequencies after mating are

$$\begin{aligned} T &= x^2 + [1 - (1-h)r]xy + \frac{y^2}{4}, \\ T &= [1 - (1-h)r]xy + 2(1-r)xz + \frac{y^2}{2} + (1-hr)yz, \\ T &= \frac{y^2}{4} + (1-hr)yz + z^2, \end{aligned} \quad (A1)$$

6 where $T = 1 - 2r[(1-h)xy + xz + hyz]$ is the sum of the frequencies of three genotypes after
7 mating (see Table 1 for the derivation). The frequencies in the next generation after viability
8 selection favoring a mutant phenotype is

$$\begin{aligned} x' &= \frac{(1+s)x}{(1+s)x + (1+hs)y + z} \\ y' &= \frac{(1+hs)y}{(1+s)x + (1+hs)y + z} \\ z' &= \frac{z}{(1+s)x + (1+hs)y + z} \end{aligned} \quad (A2)$$

10 Here we assume that A is the mutant allele and a is the wild-type allele. When $h = 1$, the
11 mutant allele is dominant; whereas, it is recessive when $h = 0$. We first consider the condition
12 for the invasion of the completely or partially dominant mutant ($0 < h \leq 1$). We then examine
13 the invasibility condition for the completely recessive mutant ($h = 0$), in which we need to
14 consult the center manifold theorem (Guckenheimer and Holmes 1983).

15

16 (i) Invasibility of the completely and partially dominant mutant ($0 < h \leq 1$)

17 We linearize the dynamics (A2) for small x and y :

$$\begin{pmatrix} x' \\ y' \end{pmatrix} = \begin{pmatrix} 0 & 0 \\ 2(1-r)(1+hs) & (1+hs)(1-hr) \end{pmatrix} \begin{pmatrix} x \\ y \end{pmatrix} \quad (A3)$$

19 The largest eigenvalue of the linearized system is $(1+hs)(1-hr)$. Thus the mutant can
20 invade if and only if $(1+hs)(1-hr) > 1$. This condition can be rewritten as $s > r / (1-hr)$.

21

22 (ii) Invasibility of the completely recessive mutant ($h = 0$)

23 If the mutant allele is completely recessive ($h = 0$), the linearized system is also
 24 given by with $h = 0$:

$$25 \quad \begin{pmatrix} x' \\ y' \end{pmatrix} = A \begin{pmatrix} x \\ y \end{pmatrix} = \begin{pmatrix} 0 & 0 \\ 2(1-r) & 1 \end{pmatrix} \begin{pmatrix} x \\ y \end{pmatrix}. \quad (\text{A4})$$

26 As the largest eigenvalue is 1, we need to have higher order terms of x and y to examine
 27 the local stability of $x = y = 0$. The Taylor expansion of (A2) up to the quadratic terms of x
 28 and y yields

$$29 \quad \begin{pmatrix} x' \\ y' \end{pmatrix} = \begin{pmatrix} 0 & 0 \\ 2(1-r) & 1 \end{pmatrix} \begin{pmatrix} x \\ y \end{pmatrix} + \begin{pmatrix} f(x, y) \\ g(x, y) \end{pmatrix}, \quad (\text{A5})$$

30 with

$$31 \quad f(x, y) = (1+s) \left[x^2 + (1-r)xy + \frac{y^2}{4} \right], \quad (\text{A6})$$

$$g(x, y) = -2(1-r)(1-2r)x^2 - (2-3r)xy - \frac{y^2}{2}.$$

32 The linear part of (A5) can be diagonalized by the transformation

$$33 \quad \begin{pmatrix} x \\ y \end{pmatrix} = P \begin{pmatrix} u \\ v \end{pmatrix}, \quad \text{with } P = \begin{pmatrix} 0 & -\frac{1}{2(1-r)} \\ 1 & 1 \end{pmatrix}, \quad (\text{A7})$$

34 where the column vectors of P are the eigenvectors corresponding to the eigenvalues 1 and
 35 0 of matrix A . This yields

$$36 \quad \begin{pmatrix} u' \\ v' \end{pmatrix} = \begin{pmatrix} 1 & 0 \\ 0 & 0 \end{pmatrix} \begin{pmatrix} u \\ v \end{pmatrix} + P^{-1} \begin{pmatrix} f(x, y) \\ g(x, y) \end{pmatrix}$$

$$\equiv \begin{pmatrix} 1 & 0 \\ 0 & 0 \end{pmatrix} \begin{pmatrix} u \\ v \end{pmatrix} + \begin{pmatrix} F(u, v) \\ G(u, v) \end{pmatrix}, \quad (\text{A8})$$

37 with

$$38 \quad F(u, v) = -\frac{1}{2}(r-s+rs)u^2 - \frac{r}{2(1-r)}uv + \frac{(2-r)r(1+s)}{2(1-r)}v^2,$$

$$G(u, v) = -\frac{1}{2}(1-r)(1+s)u^2 - \frac{(2-r)r(1+s)}{2(1-r)}v^2. \quad (\text{A9})$$

39 Define the center manifold $W^c = \{(u, v) \mid v = k(u), k'(0) = k''(0) = 0\}$ on which the trajectory

40 near $u = v = 0$ stays throughout the process. The simplest form would be $k(u) = au^2$. In
 41 order that the point (u', v') is also on the center manifold, we should have $v' = k(u')$.
 42 Substituting $u' = u + F(u, k(u))$ and $v' = G(u, k(u))$ into this yields

$$43 \quad G(u, au^2) - a[u + F(u, au^2)]^2 = 0. \quad (\text{A10})$$

44 Equating the coefficient of the leading term to zero, a is determined as

$$45 \quad a = -\frac{1}{2}(1-r)(1+s). \quad (\text{A11})$$

46 The slow dynamic of u restricted on the center manifold is then

$$47 \quad u' = u + F(u, k(u)) = u - \frac{1}{2}(r-s+rs)u^2, \quad (\text{A12})$$

48 and hence u converges to zero if $r-s+rs > 0$, or the mutant can invade if $r-s+rs < 0$
 49 (or $(1-r)(1+s) > 1$). This invasibility condition for the completely recessive mutant is
 50 equivalent to that for the completely dominant mutant, but, interestingly, differs from the
 51 condition $s > r$ in the limit of $h \rightarrow 0$ for the invasibility condition of the partially dominant
 52 mutant.

53

54

55 **Appendix S2: Invasion condition in the diploid model with delayed inheritance**

56 In the presence of delayed inheritance, a phenotype of an individual is determined by a
 57 maternal genotype. We therefore need to keep track the frequencies of 2×3 combination of
 58 phenotype \times genotype to describe the genetic dynamics. Here we denote the two alleles as
 59 A (dominant allele) and a (recessive allele). An individual has either phenotype A or a
 60 (right-handed or left-handed, depending on which is dominant) that is determined by the
 61 genotype of its mother. We denote for example an individual with the genotype AA and the
 62 phenotype A by AA_A.

63 As we assume that A is a dominant allele and a is a recessive allele in the diploid
 64 model with delayed inheritance, the genotype-phenotype combination AA_a will never be
 65 produced (indeed, for an individual to have phenotype a, its mother should be homozygote of
 66 the recessive allele, aa). We denote the frequencies of AA_A, Aa_A, Aa_a, aa_A, and aa_a as x_A , y_A ,
 67 y_a , z_A , and z_a . $x_a \equiv 0$ as noted above. The frequency of phenotype A is $x_A + y_A + z_A$ and
 68 that of phenotype a is $y_a + z_a$. Let p_i ($= x_i + y_i / 2$) be the frequency of allele A with
 69 phenotype i ($= A$ or a), and q_i ($= z_i + y_i / 2$) be the frequency of allele a with phenotype i
 70 ($= A$ or a). The frequencies after mating are calculated from Table S1 as

$$T\tilde{x}_A = (p_A + p_a)^2 - 2rp_A p_a,$$

$$T\tilde{y}_A = (p_A + p_a)(q_A + q_a) + (p_A + p_a)\frac{y_A + y_a}{2} - r(p_A q_a + p_a q_A) - \frac{r}{2}(p_a y_A + p_A y_a),$$

$$71 \quad T\tilde{y}_a = (p_A + p_a)(z_A + z_a) - r(p_a z_A + p_A z_a), \quad (B1)$$

$$T\tilde{z}_A = (q_A + q_a)\frac{y_A + y_a}{2} - \frac{r}{2}(q_a y_A + q_A y_a),$$

$$T\tilde{z}_a = (q_A + q_a)(z_A + z_a) - r(q_a z_A + q_A z_a),$$

72 where $T = 1 - 2r(x_A + y_A + z_A)(y_a + z_a)$. When there is no reproductive isolation ($r = 0$) or
 73 viability selection ($s = 0$), the ratio of two phenotypes for the heterozygous genotype, $Aa_A :$
 74 Aa_a , is $(1 + p) : (1 - p)$ and that for the homozygous genotype, $aa_A : aa_a$, is $p : (1 - p)$ under
 75 delayed inheritance assuming the HW equilibrium.

76

77 (i) Invasibility of a dominant mutant

78 The frequencies in the next generation are then given by those after the viability
 79 selection favoring a dominant handedness mutant (A) with the selection coefficient s :

$$80 \quad x'_A = \frac{(1+s)\frac{p_A}{W}}{W}, y'_A = \frac{(1+s)\frac{q_A}{W}}{W}, y'_a = \frac{\frac{q_a}{W}}{W}, z'_A = \frac{(1+s)\frac{p_A}{W}}{W}, z'_a = \frac{\frac{q_a}{W}}{W}, \quad (B1)$$

81 where $W = 1 + s(\tilde{x}_A + \tilde{y}_A + \tilde{z}_A)$ is the mean fitness of the population.

82 We now examine the invasibility of the dominant allele A in the resident population
 83 consisting only of the recessive allele a (i.e., $z_a = 1$ and $x_A = y_A = y_a = z_A = 0$). The
 84 system **Error! Reference source not found.**-(B1) is linearized with respect to $z_A, y_A, y_a,$
 85 and x_A as

$$86 \quad \begin{pmatrix} z'_A \\ y'_a \\ y'_A \\ x'_A \end{pmatrix} = \begin{pmatrix} 0 & (1+s)/2 & (1-r)(1+s)/2 & 0 \\ 0 & 1/2 & (1-r)/2 & 1-r \\ 0 & (1+s)/2 & (1-r)(1+s)/2 & (1-r)(1+s) \\ 0 & 0 & 0 & 0 \end{pmatrix} \begin{pmatrix} z_A \\ y_a \\ y_A \\ x_A \end{pmatrix}, \quad (B2)$$

87 where z_a is eliminated by using $z_a = 1 - x_A - y_A - y_a - z_A$. The Jacobian matrix in the right
 88 hand side of (B2) has three zero eigenvalues and a non-trivial eigenvalue,

$$89 \quad \lambda = \frac{1}{2}(2 + s - r - rs). \quad (B3)$$

90 The population allows the invasion of the dominant mutant if $\lambda > 1$, which gives exactly the
 91 same condition $(1-r)(1+s) > 1$ as that for the invasibility of dominant mutant if there was
 92 no delayed inheritance. Though the condition for the invasibility is the same, the value (B3)

93 itself is smaller than the dominant eigenvalue, $\lambda' = (1-r)(1+s)$, when there was no delayed
 94 inheritance, which corresponds to the fact that the delayed inheritance makes the invasion of a
 95 handedness mutant easier in a finite population.

96

97 **(ii) Invasibility of a recessive mutant**

98 Let us now consider the invasibility of a recessive handedness mutant that enjoys an
 99 ecological advantage in viability with the selection coefficient s . The frequencies after
 100 reproduction are given by **Error! Reference source not found.**, and the frequencies in the
 101 next generation are

$$102 \quad x'_A = \frac{\tilde{x}_A}{W}, y'_A = \frac{\tilde{y}_A}{W}, y'_a = \frac{(1+s)\tilde{y}_a}{W}, z'_A = \frac{\tilde{z}_A}{W}, z'_a = \frac{(1+s)\tilde{z}_a}{W}, \quad (B4)$$

103 where $W = 1 + s(\tilde{y}_a + \tilde{z}_a)$ is the mean fitness. As before $\tilde{x}_a = 0$. The resident population
 104 consists only of dominant allele A (i.e., $x_A = 1$ and $y_A = y_a = z_A = z_a = 0$). The system
 105 **Error! Reference source not found.**, (B4) is linearized with respect to $z_a, z_A, y_a,$ and
 106 y_A as

$$107 \quad \begin{pmatrix} z'_a \\ z'_A \\ y'_a \\ y'_A \end{pmatrix} = A \begin{pmatrix} z_a \\ z_A \\ y_a \\ y_A \end{pmatrix} + \begin{pmatrix} f_1(z_a, z_A, y_a, y_A) \\ f_2(z_a, z_A, y_a, y_A) \\ f_3(z_a, z_A, y_a, y_A) \\ f_4(z_a, z_A, y_a, y_A) \end{pmatrix} \quad (B5)$$

$$= \begin{pmatrix} 0 & 0 & 0 & 0 \\ 0 & 0 & 0 & 0 \\ (1-r)(1+s) & 1+s & 0 & 0 \\ 1-r & 1 & 1-r & 1 \end{pmatrix} \begin{pmatrix} z_a \\ z_A \\ y_a \\ y_A \end{pmatrix} + \begin{pmatrix} f_1(z_a, z_A, y_a, y_A) \\ f_2(z_a, z_A, y_a, y_A) \\ f_3(z_a, z_A, y_a, y_A) \\ f_4(z_a, z_A, y_a, y_A) \end{pmatrix},$$

108 where f_i 's are quadratic or higher order terms of $z_a, z_A, y_a,$ and y_A . The matrix A has
 109 eigenvalues $\lambda = 1$ and $\lambda = 0$ (with multiplicity 3). Because the dominant eigenvalue is 1,
 110 we need to construct a center manifold to examine the local stability of the equilibrium

111 $(z_a, z_A, y_a, y_A)^T = (0, 0, 0, 0)^T$, where superscript T denotes the vector transform.

112 The eigenvector corresponding to the eigenvalue 1 is found, by solving

113 $(A - I)\mathbf{b} = \mathbf{0}$, to be $\mathbf{b}_1 = (1, 0, 0, 0)^T$, where I is a 4×4 identity matrix. There are two

114 eigenvectors satisfying $(A - 0I)\mathbf{b} = A\mathbf{b} = \mathbf{0}$ corresponding to the eigenvalue 0:

115
$$\mathbf{b}_2 = \begin{pmatrix} 1 \\ -(1-r) \\ 0 \\ 0 \end{pmatrix}, \text{ and } \mathbf{b}_3 = \begin{pmatrix} 0 \\ 0 \\ 1 \\ -(1-r) \end{pmatrix}. \quad (\text{B6})$$

116 We now find a nonzero vector \mathbf{b}_4 that, together with \mathbf{b}_2 and \mathbf{b}_3 , spans the 3-dimensional
 117 generalized eigenspace corresponding to the eigenvalue 0. Such vector \mathbf{b}_4 must satisfy

118 $(A-0I)^2\mathbf{b}_4 = A^2\mathbf{b}_4 = \mathbf{0}$ and be linearly independent of \mathbf{b}_2 or \mathbf{b}_3 , which is obtained as

119
$$\mathbf{b}_4 = \begin{pmatrix} 1 \\ 0 \\ 0 \\ -(1-r)(2+s-r-rs) \end{pmatrix}. \quad (\text{B7})$$

120 Now we define the transformation matrix P whose columns consist of \mathbf{b}_1 , \mathbf{b}_2 , \mathbf{b}_3 , and
 121 \mathbf{b}_4 :

122
$$P = \begin{pmatrix} 0 & 1 & 0 & 1 \\ 0 & -(1-r) & 0 & 0 \\ 0 & 0 & 1 & 0 \\ 1 & 0 & -(1-r) & -(1-r)(2+s-r-rs) \end{pmatrix}. \quad (\text{B8})$$

123 We then transform the variables as

124
$$\begin{pmatrix} z_a \\ z_A \\ y_a \\ y_A \end{pmatrix} = P \begin{pmatrix} u_1 \\ u_2 \\ u_3 \\ u_4 \end{pmatrix}. \quad (\text{B9})$$

125 The dynamics for the transformed variables become

$$\begin{pmatrix} u'_1 \\ u'_2 \\ u'_3 \\ u'_4 \end{pmatrix} = P^{-1}AP \begin{pmatrix} u_1 \\ u_2 \\ u_3 \\ u_4 \end{pmatrix} + P^{-1} \begin{pmatrix} f_1 \\ f_2 \\ f_3 \\ f_4 \end{pmatrix} \tag{B10}$$

$$= \begin{pmatrix} 1 & 0 & 0 & 0 \\ 0 & 0 & 0 & 0 \\ 0 & 0 & 0 & (1-r)(1+s) \\ 0 & 0 & 0 & 0 \end{pmatrix} \begin{pmatrix} u_1 \\ u_2 \\ u_3 \\ u_4 \end{pmatrix} + \begin{pmatrix} F_1(u_1, u_2, u_3, u_4) \\ F_2(u_1, u_2, u_3, u_4) \\ F_3(u_1, u_2, u_3, u_4) \\ F_4(u_1, u_2, u_3, u_4) \end{pmatrix}.$$

127 Here, $F_i(u_1, u_2, u_3, u_4)$ is the i th row of $P^{-1}\mathbf{f}(\mathbf{x}) = P^{-1}\mathbf{f}(P\mathbf{u})$ where $\mathbf{f} = (f_1, f_2, f_3, f_4)^T$,

128 $\mathbf{x} = (z_a, z_A, y_a, y_A)^T$, and $\mathbf{u} = (u_1, u_2, u_3, u_4)^T$. We now define the center manifold

$$W^c = \{(u_1, u_2, u_3, u_4) \mid u_2 = f(u_1), u_3 = g(u_1), u_4 = h(u_1)\}, \tag{B11}$$

130 where f , g , and h are functions with the following properties: $f(0) = g(0) = h(0) = 0$

131 and $f'(0) = g'(0) = h'(0) = 0$. The simplest forms for such functions are $f(u) = au^2$,

132 $g(u) = bu^2$, and $h(u) = cu^2$ where a , b , and c are constants. Substituting these into

133 (B10), and requiring that the variables u'_2 , u'_3 , and u'_4 in the next generation must lie on the

134 center manifold ($u'_2 = f(u'_1)$, $u'_3 = g(u'_1)$, and $u'_4 = h(u'_1)$), we now have

$$\begin{aligned}
u'_1 &= u_1 + F_1(u_1, au_1^2, bu_1^2, cu_1^2), \\
a[u_1 + F_1(u_1, au_1^2, bu_1^2, cu_1^2)]^2 &= F_2(u_1, au_1^2, bu_1^2, cu_1^2), \\
b[u_1 + F_1(u_1, au_1^2, bu_1^2, cu_1^2)]^2 &= (1-r)(1+s)cu_1^2 + F_3(u_1, au_1^2, bu_1^2, cu_1^2), \\
c[u_1 + F_1(u_1, au_1^2, bu_1^2, cu_1^2)]^2 &= F_4(u_1, au_1^2, bu_1^2, cu_1^2).
\end{aligned} \tag{B12}$$

136 The coefficients a , b , and c are determined from the leading order terms of the second to

137 the forth equations of (B12) as

$$a = -\frac{1}{4(1-r)}, \quad b = \frac{1+s}{4}, \quad c = \frac{1}{4(1-r)}. \tag{B13}$$

139 Substituting this into the first equation of (B12), we have a slow dynamics on the center

140 manifold:

141
$$u_1' = u_1 + \frac{1}{4}(s - r - rs)u_1^2 + O(u_1^3). \quad (\text{B14})$$

142 Thus, u_1 converges to zero if and only if $s(1-r) - r < 0$ or $s < r/(1-r)$. Conversely, the
 143 recessive mutant can invade the population if $s > r/(1-r)$. This condition is the same as the
 144 condition $(2+s-r-rs)/2 > 1$ or $(1-r)(1+s) > 1$ for the invasibility of the dominant
 145 mutant.

146 The center manifold $u_2 = -u_1^2/[4(1-r)]$, $u_3 = (1+s)u_1^2/4$, and $u_4 = u_1^2/[4(1-r)]$
 147 in the original coordinate is defined in a parametric form with a parameter $\xi = u_1$ as

148
$$\begin{aligned} z_a &= O(\xi^3), \\ z_A &= \frac{1}{4}\xi^2 + O(\xi^3), \\ y_a &= \frac{1+s}{4}\xi^2 + O(\xi^3), \\ y_A &= \xi - \frac{3+2s-2r-2rs}{4}\xi^2 + O(\xi^3). \end{aligned} \quad (\text{B15})$$

149

150

151 **Appendix S3: Diffusion approximation analysis of the diploid model without delayed**
 152 **inheritance**

153 We here derive the approximate one-dimensional diffusion process describing the allele
 154 frequency dynamics in a finite population of effective population size N without delayed
 155 inheritance. The discrete-generation genotype dynamics in infinite population are derived as
 156 (A1)-(A2) of Appendix S1. As is usual in diffusion approximation, we take the limit of weak
 157 fecundity and viability selections, $r \rightarrow 0$, $s \rightarrow 0$, and large population $N \rightarrow \infty$ with the
 158 products Nr and Ns being kept finite.

159 Assuming that both s and r are of the order of ε , a small positive constant, we
 160 expand the dynamics (A1)-(A2) in Taylor series with respect to ε . The leading order dynamics
 161 for the zygote frequencies x , y , and z of genotypes AA, Aa, and aa are then

162
$$\begin{aligned} x' &= p^2 + O(\varepsilon), \\ y' &= 2pq + O(\varepsilon), \\ z' &= q^2 + O(\varepsilon), \end{aligned} \quad (\text{C1})$$

163 where $p = x + y/2$ and $q = z + y/2$ respectively is the frequency of allele A and a. Thus,
 164 in the leading order, genotype frequencies are in the Hardy-Weinberg equilibrium. From this it

165 also follows that the allele frequencies do not change with time, $p' = p$ and $q' = q$, up to
 166 the leading order.

167 Now we derive the slow allele frequency dynamics as the first order expansion of
 168 the equations (A1) and (A2). The change in the allele frequency p of the mutant allele A is
 169 then

$$170 \quad \Delta p = p(1-p) \left\{ r \left[p(2p^2 - 1) - h(6p^2 - 6p + 1) \right] + s \left[p + h(1 - 2p) \right] \right\} + O(\varepsilon^2). \quad (C2)$$

171 Note that s in (C2) is the selection coefficient favoring the phenotype A. From (C2) we have
 172 the frequency dynamics:

$$173 \quad \dot{p} = p(1-p) \left\{ r \left[p(2p^2 - 1) - h(6p^2 - 6p + 1) \right] + s \left[p + h(1 - 2p) \right] \right\} \quad (C3)$$

174 The dynamics has two stable equilibria at $p = 0$ and $p = 1$, and an internal unstable
 175 equilibrium when $r > s$.

176 With random genetic drift, the diffusion process for the change in the allele
 177 frequency is characterized by infinitesimal mean and variance of the frequency change:

$$178 \quad \begin{aligned} M(p) &= E[\Delta p | p] = p(1-p) \left\{ r \left[p(2p^2 - 1) - h(6p^2 - 6p + 1) \right] + s \left[p + h(1 - 2p) \right] \right\}, \\ V(p) &= E[(\Delta p)^2 | p] = \frac{p(1-p)}{2N}. \end{aligned} \quad (C4)$$

179 The fixation probability of the allele A with the initial frequency p then satisfies the
 180 backward equation (12) with the boundary condition $u(0) = 0$ and $u(1) = 1$. This yields
 181 equation (13). The fixation probability of a single mutant $\rho = u(1/2N)$ is then

$$182 \quad \rho = \frac{1/(2N)}{\int_0^1 \exp \left\{ 4Nry(1-y) \left[\frac{y}{2}(1+y) - h(2y-1) \right] - 4Nsy \left[\frac{y}{2} + h(1-y) \right] \right\} dy}, \quad (C5)$$

183 The relative fixation rate of a single mutant relative to that of a neutral mutant is given by
 184 $\phi = 2N\rho$:

$$185 \quad \phi = \frac{1}{\int_0^1 \exp \left\{ Ry(1-y) \left[\frac{y}{2}(1+y) - h(2y-1) \right] - Sy \left[\frac{y}{2} + h(1-y) \right] \right\} dy}, \quad (C6)$$

186 where $R = 4Nr$ and $S = 4Ns$. Here we consider three cases: (i) $h = 0$ (the recessive mutant),
 187 (ii) $h = 1$ (the dominant mutant), (iii) $h = 0.5$ (the partially dominant mutant).

188

189 **(i) $h = 0$ (the recessive mutant)**

190 After factorization, the deterministic dynamics is

191
$$\dot{p} = p^2(1-p)[r(2p^2-1)+s], \quad (C7)$$

192 when $h = 0$. This can be written as

193
$$\dot{p} = 2rp^2(1-p)\left(p - \sqrt{\frac{r-s}{2r}}\right)\left(p + \sqrt{\frac{r-s}{2r}}\right),$$

194 when $r > 0$ and $r > s$. Thus the dynamics has an internal unstable equilibrium at
 195 $p_c = \sqrt{(r-s)/2r}$ when $r > s$. When $s = 0$, therefore, the dynamics has two stable equilibria at
 196 $p = 0$ and $p = 1$, and an internal unstable equilibrium at $p_c = 1/\sqrt{2}$ (the dotted blue line in
 197 Fig. 3).

198 The relative fixation rate is

199
$$\phi_0 = \frac{1}{\int_0^1 \exp\left\{\frac{y^2}{2}[R(1-y^2)-S]\right\} dy}. \quad (C8)$$

200 When $s = 0$, for the relative fixation rate, $\phi_0 = 1 / \int_0^1 \exp\left[\frac{Ry^2}{2}(1-y^2)\right] dy$, we can show the
 201 following properties. Firstly, at the limit of $R \rightarrow 0$ the fixation probability is equal to that of
 202 a neutral allele:

203
$$\phi_0|_{R=0} = 1. \quad (C9)$$

204 Secondly we see that $1/\phi_0$ is convex with respect to R because

205
$$\frac{\partial^2}{\partial R^2} \left(\frac{1}{\phi_0} \right) = \frac{1}{4} \int_0^1 (y^2 - y^4)^2 \exp\left[\frac{R}{2}(y^2 - y^4)\right] dy > 0. \quad (C10)$$

206 Thirdly we see that the sign of the initial slope of $1/\phi_0$ from

207
$$\left. \frac{\partial}{\partial R} \left(\frac{1}{\phi_0} \right) \right|_{R=0} = \frac{1}{15}. \quad (C11)$$

208 Because the right-hand side of equation (C11) is positive, ϕ_0 is smaller than 1 for any $R > 0$.
 209 The fixation probability of a dominant mutant allele is always smaller than that, $1/(2N)$, of a
 210 neutral allele (i.e. the native recessive allele is the finite population size ESS, ESS_N , in the
 211 sense of Nowak et al. (2004)). In addition, this value is smaller than the haploid model ($1/12$),
 212 implying that the reduction rate of fixation probability is more moderate in the diploid model.

213

214 **(ii) $h = 1$ (the dominant mutant)**

215 The frequency dynamics of dominant mutant is obtained from equation (C3):

216
$$\dot{p} = p(1-p)^2 \left[-r(2p^2 - 4p + 1) + s \right]. \quad (\text{C12})$$

217 This can be written as

218
$$\dot{p} = 2rp(1-p)^2 \left[p - \left(1 - \sqrt{\frac{r+s}{2r}} \right) \right] \left[\left(1 + \sqrt{\frac{r+s}{2r}} \right) - p \right].$$

219 If $r > s$, this has an internal unstable equilibrium at $p_c = 1 - \sqrt{(r+s)/2r}$. When $s = 0$, the
 220 dynamics has an internal unstable equilibrium at $p_c = 1 - 1/\sqrt{2}$ (the dotted red line in Fig. 3).

221 Therefore the relative fixation rate of a recessive mutant to that of a neutral allele
 222 $\phi_1 = 2N\rho_1$ then satisfies

223
$$\phi_1 = \frac{1}{\int_0^1 \exp \left\{ \frac{y}{2} (2-y) [R(1-y)^2 - S] \right\} dy}. \quad (\text{C13})$$

224 If $s = 0$, we can show that the function $(1/\phi_1)$ is convex with respect to R , $\phi_1|_{R=0} = 1$, and

225 $(\partial(1/\phi_1)/\partial R)|_{R=0} = 1/15$. Actually, ϕ_1 and ϕ_0 are equivalent ($\phi_0 = \phi_1$) when $s = 0$, though

226 it is different when $s > 0$. This is obvious from equations (C8) and (C13); if we represent the

227 frequency of the recessive allele as p and that of the dominant allele as q , then

228
$$\begin{aligned} p^2(1-p^2) &= (1-q)^2 [1 - (1-q)^2] \\ &= q(2-q)(1-q)^2. \end{aligned} \quad (\text{C14})$$

229

230 **(iii) $h = 0.5$ (the partially dominant mutant)**

231 The frequency dynamics of mutant with partial dominance is obtained from
 232 equation (C3):

233
$$\dot{p} = \frac{1}{2} p(1-p) \left[r(2p-1)(2p^2 - 2p + 1) + s \right]. \quad (\text{C15})$$

234 This has an internal unstable equilibrium at

235
$$p_c = \frac{1}{2} + \frac{1}{2} \left(\sqrt{\frac{1}{27} + \left(\frac{s}{r}\right)^2} - \frac{s}{r} \right)^{\frac{1}{3}} - \frac{1}{6} \left(\sqrt{\frac{1}{27} + \left(\frac{s}{r}\right)^2} - \frac{s}{r} \right)^{\frac{1}{3}},$$

236 when $r > s$. Equation (C15) has an internal unstable equilibrium at $p_c = 1/2$ when $s = 0$ (the
 237 dotted lime-green line in Fig. S1). The relative fixation rate is

$$238 \quad \phi_2 = \frac{1}{\int_0^1 \exp \left\{ \frac{y}{2} [R(1-2y+2y^2-y^3)-S] \right\} dy}. \quad (\text{C16})$$

239 If $s = 0$, we can show that the function $(1/\phi_2)$ is convex with respect to R , $\phi_2|_{R=0} = 1$, and
 240 $(\partial(1/\phi_2)/\partial R)|_{R=0} = 1/15$.

241 These analytical expressions for the relative fixation rates ϕ_0 , ϕ_1 and ϕ_2
 242 obtained from one-dimensional diffusion approximation showed good agreements with the
 243 simulation results when $N = 1,000$ (Fig. 4H). When $s = 0$, we found that ϕ_0 and ϕ_1 are
 244 equivalent as shown in equation (C14) (Fig. 4H) and that ϕ_2 is higher than ϕ_0 and ϕ_1
 245 when R is not small, implying that partial dominance can promote fixation of the mutant
 246 allele in the diploid model with three phenotypes (Figs. 4H, S2C).

247
 248

249 **Appendix S4: Diffusion approximation analysis of the diploid model with delayed** 250 **inheritance**

251 We here derive the approximate one-dimensional diffusion process describing the allele
 252 frequency dynamics of snail handedness alleles in a finite population of effective population
 253 size N with delayed inheritance. The discrete-generation genotype-phenotype dynamics in
 254 infinite population are derived as (B1) and (B2) or (B1) and (B5) of Appendix S2. As is usual
 255 in diffusion approximation, we take the limit of weak fecundity and viability selections,
 256 $r \rightarrow 0$, $s \rightarrow 0$, and large population $N \rightarrow \infty$ with the products Nr and Ns being kept
 257 finite.

258 Assuming that both s and r are of the order of ε , a small positive constant, we
 259 expand the dynamics (B1) and (B2)/(B5) in Taylor series with respect to ε . The leading
 260 order dynamics for the zygote frequencies $x = x_A + x_a$, $y = y_A + y_a$, $z = z_A + z_a$ of
 261 genotypes AA, Aa, and aa are then

$$262 \quad \begin{aligned} x' &= p^2 + O(\varepsilon), \\ y' &= 2pq + O(\varepsilon), \\ z' &= q^2 + O(\varepsilon), \end{aligned} \quad (\text{D1})$$

263 where $p = x + y/2$ and $q = z + y/2$ respectively is the frequency of allele A and a. Thus,
 264 in the leading order, genotype frequencies are in the Hardy-Weinberg equilibrium. From this it

265 also follows that the allele frequencies do not change with time, $p' = p$ and $q' = q$, up to
 266 the leading order. The frequencies of phenotype-genotype combinations are thus kept constant
 267 for a given allele frequency p (or q) up to the leading order:

$$\begin{aligned}
 x_A &= p^2 + O(\varepsilon), \\
 x_a &= 0, \\
 y_A &= pq(1+p) + O(\varepsilon), \\
 y_a &= pq^2 + O(\varepsilon), \\
 z_A &= pq^2 + O(\varepsilon), \\
 z_a &= q^3 + O(\varepsilon).
 \end{aligned}
 \tag{D2}$$

269 Now we derive the slow allele frequency dynamics as the first order expansion of
 270 the equations (B1) and (B2)/(B5). The change in the allele frequency p of the dominant
 271 allele A is then

$$\Delta p = \frac{1}{2} p(1-p)^2 [-r(2p^2 - 4p + 1) - s] + O(\varepsilon^2).
 \tag{D3}$$

273 For the frequency q of the recessive allele, we have

$$\Delta q = \frac{1}{2} q^2(1-q) [r(2q^2 - 1) + s] + O(\varepsilon^2).
 \tag{D4}$$

275 Note that s in (D3) and (D4) is the selection coefficient favoring phenotype a. If phenotype
 276 A is selected for, the sign must be changed before s in the right hand side of (D3) and (D4).
 277

278 (i) The dominant mutant alleles

279 If the dominant mutant is selected for in the viability selection, we change the sign
 280 before s in the right hand side of (D3) to have the deterministic dynamics,

$$\dot{p} = \frac{1}{2} p(1-p)^2 [-r(2p^2 - 4p + 1) + s].
 \tag{D5}$$

282 This rate of change in the allele frequency of dominant allele is exactly a half of that for the
 283 diploid model without delayed inheritance with $h = 1$ (eq. C12). In other words, the delayed
 284 inheritance does not change allele frequency dynamics at all except for its halved rate.
 285 Therefore, the position of internal unstable equilibrium, $p_c = 1 - 1/\sqrt{2}$, is the same as in the
 286 model without delayed inheritance (the solid red line in Fig. 3).

287 The relative fixation rate of a dominant mutant to that of a neutral allele
 288 $\phi_A = 2N\rho_A$ then satisfies

289
$$\phi_A = \frac{1}{\int_0^1 \exp \left\{ \frac{y}{4} (2-y) [R(1-y)^2 - S] \right\} dy}. \quad (\text{D6})$$

290

291 **(ii) The recessive mutant allele**

292 If the recessive allele is selected for in the viability selection, we have from (D4) the
 293 deterministic dynamics,

294
$$\dot{q} = \frac{1}{2} q^2 (1-q) [r(2q^2 - 1) + s]. \quad (\text{D7})$$

295 Again, the right hand side is exactly a half of that for the diploid model without delayed
 296 inheritance with $h = 0$ (eq. C7). Thus, two stable equilibria at $q = 0$ and $q = 1$, and an internal
 297 unstable equilibrium at $q_c = 1/\sqrt{2}$ are exactly the same as in the model without delayed
 298 inheritance (the solid blue line in Fig. 3). The relative fixation rate of a recessive mutant to
 299 that of a neutral allele $\phi_a = 2N\rho_a$ then satisfies

300
$$\phi_a = \frac{1}{\int_0^1 \exp \left\{ \frac{z^2}{4} [R(1-z^2) - S] \right\} dz}. \quad (\text{D8})$$

301 Note that ϕ_A and ϕ_a are equivalent when $s = 0$, which can be shown by changing the
 302 variables in the integral in (D8) from z to $y = 1 - z$. When $s = 0$, the initial slope of $1/\phi_A$
 303 and $1/\phi_a$ is $(\partial(1/\phi_A)/\partial R)|_{R=0} = 1/30$. This value is smaller than the haploid model (1/12)
 304 and the diploid model without delayed inheritance (1/15), implying that the reduction rate of
 305 fixation probability is more moderate in the diploid model with delayed inheritance.

306 The analytical formula for the relative fixation probabilities, (D6) and (D8), by one
 307 dimensional diffusion approximation showed good agreements with the Monte Carlo
 308 simulation results for the original 4 dimensional genotype-phenotype dynamics for
 309 sufficiently large N ($N = 1,000$, Fig. 4I).

310

311

312 **Appendix S5: Exact fixation probabilities in the haploid model**

313 We calculated exact fixation probabilities in the Markov process without any approximation
 314 by the first step analysis. Consider a finite population with N haploid individuals. Recursion
 315 equations of fixation probabilities can be written as

316

$$u(i) = \sum_{j=0}^N P_{i,j} u(j), \quad (\text{E1})$$

317 where $u(i)$ is the probability that a mutant allele starting with i individuals in the initial
 318 population eventually goes to fixation, and $P_{i,j}$ is the transition probability that the number of
 319 mutant allele change from i to j in one generation ($0 \leq i, j \leq N$). Note that u here is a function
 320 of number of individuals, but u in Appendix S3 and S4 is a function of frequencies. With the
 321 boundary conditions $u(0) = 0$ and $u(N) = 1$, the fixation probability can be obtained by solving
 322 linear equations with $N - 1$ unknown variables. This can be written in a matrix form:

323

$$\mathbf{A}\mathbf{u} = \mathbf{b}, \quad (\text{E2})$$

324 where

325

$$\mathbf{A} = \begin{pmatrix} P_{1,1} - 1 & P_{1,2} & \text{L} & P_{1,(N-1)} \\ P_{2,1} & P_{2,2} - 1 & \text{L} & P_{2,(N-1)} \\ \text{M} & \text{M} & \text{O} & \text{M} \\ P_{(N-1),1} & P_{(N-1),2} & \text{L} & P_{(N-1),(N-1)} - 1 \end{pmatrix},$$

$$\mathbf{u} = \begin{pmatrix} u(1) \\ u(2) \\ \text{M} \\ u(N-1) \end{pmatrix},$$

$$\mathbf{b} = \begin{pmatrix} -P_{1,N} \\ -P_{2,N} \\ \text{M} \\ -P_{(N-1),N} \end{pmatrix}.$$

326 The solution can be obtained by multiplying the inverse of matrix A in the both sides of
 327 (E1): $\mathbf{u} = \mathbf{A}^{-1}\mathbf{b}$. The transition probability $P_{i,j}$ is given by the binomial distribution when
 328 there is no selection ($r = s = 0$):

329

$$P_{i,j} = \binom{N}{j} p^j (1-p)^{N-j}, \quad (\text{E3})$$

330 where $p = i/N$. When there is positive frequency-dependent selection due to reproductive
 331 isolation ($r > 0$ and $s = 0$), the expected frequency in the next generation in equation (E3), p ,
 332 is replaced by equation (1):

333

$$P_{i,j} = \binom{N}{j} \left(\frac{p[1-r(1-p)]}{1-2rp(1-p)} \right)^j \left(1 - \frac{p[1-r(1-p)]}{1-2rp(1-p)} \right)^{N-j}. \quad (\text{E4})$$

334 When there is viability selection for the mutant ($r > 0$ and $s > 0$), equation (E3) is replaced by

$$335 \quad P_{i,j} = \binom{N}{j} \left(\frac{(1+s)\tilde{p}_0}{1+s\tilde{p}_0} \right)^j \left(1 - \frac{(1+s)\tilde{p}_0}{1+s\tilde{p}_0} \right)^{N-j}, \quad (\text{E5})$$

336 where \tilde{p} is from equation (1). The graphs of $u(1)$ are in good agreement with the simulation
337 results when $N = 3$ (Fig. 4A).

338 One drawback of this method is that calculating the inverse matrix of the transition
339 probability matrix, A , is time-consuming or almost impossible when N is large. In the
340 diploid models, the dimension is two without delayed inheritance and four with delayed
341 inheritance. Due to the ‘curse of dimensionality,’ therefore, calculation is especially difficult
342 in the diploid models. For sufficiently small population size, however, this method is practical
343 and gives accurate results for very small N when diffusion approximation fails.

344

345

346 **Appendix S6: Exact fixation probabilities in the diploid model without delayed** 347 **inheritance**

348 Consider a finite population with diploid N individuals. The fixation probability can be
349 calculated as

$$350 \quad u(i, j) = \sum_{k=0}^N \sum_{l=0}^N P_{ij,kl} u(k, l), \quad (\text{F1})$$

351 where $u(i, j)$ is the fixation probability when there are i individuals of AA homozygote and j
352 individuals of aa homozygote (we call this as state (i, j) hereafter) and $P_{ij,kl}$ is the transition
353 probability from state (i, j) to state (k, l) in one generation ($0 \leq i, j, k, l \leq N$). Note that the
354 number of heterozygous individuals Aa is $(N - i - j)$ or $(N - k - l)$. With the boundary
355 conditions $u(0, N) = 0$ and $u(N, 0) = 1$ where the mutant allele is A and the wild-type allele is
356 a, the fixation probability of a mutant allele, $u(0, N - 1)$, can be obtained by solving linear
357 equations for $(N + 1)(N + 2) / 2 - 2$ unknowns $u(i, j)$ for $i = 0, 1, \dots, N - 1$,
358 $j = 0, 1, \dots, N - 1$, with $i + j \leq N$. This can be rewritten in a matrix form $\mathbf{A}\mathbf{u} = \mathbf{b}$:

$$359 \quad \begin{pmatrix} P_{00,00} - 1 & P_{00,01} & \text{L} & P_{00,(N-1)l} \\ P_{01,00} & P_{01,01} - 1 & \text{L} & P_{01,(N-1)l} \\ \text{M} & \text{M} & \text{O} & \text{M} \\ P_{(N-1)l,00} & P_{(N-1)l,01} & \text{L} & P_{(N-1)l,(N-1)l} - 1 \end{pmatrix} \begin{pmatrix} u(0,0) \\ u(0,1) \\ \text{M} \\ u(N-1,1) \end{pmatrix} = \begin{pmatrix} -P_{00,N0} \\ -P_{01,N0} \\ \text{M} \\ -P_{(N-1)l,N0} \end{pmatrix}.$$

360 The solution is obtained by multiplying the inverse of matrix A in the both sides: $\mathbf{u} = A^{-1}\mathbf{b}$.

361 The transition probability is given by the multinomial distribution,

362
$$P_{ij,kl} = \frac{N!}{k!(N-k-l)!l!} \left[\left(x + \frac{y}{2} \right)^2 \right]^k \left[2 \left(x + \frac{y}{2} \right) \left(\frac{y}{2} + z \right) \right]^{N-k-l} \left[\left(\frac{y}{2} + z \right)^2 \right]^l, \quad (\text{F2})$$

363 where $x = i/N$, $y = 1 - (i + j)/N$, and $z = j/N$. When there is positive frequency-dependent
 364 selection due to reproductive isolation or viability selection for the mutant in addition to
 365 reproductive isolation, the expected frequencies of genotypes in the next generation in
 366 equation (F2) is replaced by equation (A1) or (A2).

367

368

369 **Appendix S7: Exact fixation probabilities in the diploid model with delayed inheritance**

370 Consider a finite population with diploid N individuals. The fixation probability can be
 371 calculated as

372
$$u(a,b,c,d) = \sum_{i=0}^N \sum_{j=0}^N \sum_{k=0}^N \sum_{l=0}^N P_{abcd,ijkl} u(i,j,k,l), \quad (\text{G1})$$

373 where $u(a, b, c, d)$ is the fixation probability when there are a individuals of AA_A , b
 374 individuals of Aa_A , c individuals of Aa_a , and d individuals of aa_A (we call this as state $(a, b, c,$
 375 $d)$ hereafter) and $P_{abcd,ijkl}$ is the transition probability from state (a, b, c, d) to state (i, j, k, l) in
 376 one generation ($0 \leq a, b, c, d, i, j, k, l \leq N$). Note that the number of aa_a individuals is $(N - a -$
 377 $b - c - d)$ or $(N - i - j - k - l)$. The frequencies of AA_A , Aa_A , Aa_a , and aa_A are $x_A (= a/N)$, y_A
 378 $(= b/N)$, $y_a (= c/N)$, $z_A (= d/N)$. With the boundary conditions $u(0, 0, 0, 0) = u(0, 0, 0, 1) = \dots =$
 379 $u(0, 0, 0, N) = 0$ and $u(N, 0, 0, 0) = 1$ where the dominant mutant allele is A and the recessive
 380 wild-type allele is a , the fixation probability of a mutant allele, $u(0, 0, 1, 0)$, can be obtained
 381 by solving linear equations for $u(i, j, k, l)$ with $i, j, k, l = 0, 1, \dots, N$ and $i + j + k + l \leq N$.

382 This can be rewritten in a matrix form $\mathbf{A}\mathbf{u} = \mathbf{b}$:

383
$$\begin{pmatrix} P_{1000,1000} - 1 & P_{1000,2000} & \text{L} & P_{1000,00N0} \\ P_{2000,1000} & P_{2000,2000} - 1 & \text{L} & P_{2000,00N0} \\ \text{M} & \text{M} & \text{O} & \text{M} \\ P_{00N0,1000} & P_{00N0,2000} & \text{L} & P_{00N0,00N0} - 1 \end{pmatrix} \begin{pmatrix} u(1,0,0,0) \\ u(2,0,0,0) \\ \text{M} \\ u(0,0,N,0) \end{pmatrix} = \begin{pmatrix} -P_{1000,N000} \\ -P_{2000,N000} \\ \text{M} \\ -P_{00N0,N000} \end{pmatrix}.$$

384 The solution is obtained as: $\mathbf{u} = \mathbf{A}^{-1}\mathbf{b}$. The transition probability is given by the multinomial
 385 distribution,

386
$$P_{abcd,ijkl} = \frac{N!}{i!j!k!l!(N-i-j-k-l)!} \bar{x}_A^i \bar{y}_A^j \bar{y}_a^k \bar{z}_A^l (1 - \bar{x}_A - \bar{y}_A - \bar{y}_a - \bar{z}_A)^{N-i-j-k-l}, \quad (\text{G2})$$

387 where

$$\begin{aligned}\bar{x}_A &= \left(\frac{a}{N} + \frac{b+c}{2N} \right)^2, \\ \bar{y}_A &= \left(\frac{a}{N} + \frac{b+c}{2N} \right) \left(1 - \frac{a}{N} \right), \\ \bar{y}_a &= \left(\frac{a}{N} + \frac{b+c}{2N} \right) \frac{d+e}{N}, \\ \bar{z}_A &= \frac{b+c}{2N} \left(\frac{b+c}{2N} + \frac{d+e}{N} \right).\end{aligned}$$

388

389 The expected frequencies in the next generation in equation (G2) are replaced by equations
390 (B1)-(B2) when there is positive frequency-dependent selection due to reproductive isolation
391 and viability selection for the mutant.

392 When the recessive mutant allele is a and the wild-type allele is A, we solved the
393 equation,

$$394 \begin{pmatrix} P_{1000,1000} - 1 & P_{1000,2000} & L & P_{1000,00N0} \\ P_{2000,1000} & P_{2000,2000} - 1 & L & P_{2000,00N0} \\ M & M & O & M \\ P_{00N0,1000} & P_{00N0,2000} & L & P_{00N0,00N0} - 1 \end{pmatrix} \begin{pmatrix} u(1,0,0,0) \\ u(2,0,0,0) \\ M \\ u(0,0,N,0) \end{pmatrix} = \begin{pmatrix} -P_{1000,0000} \\ -P_{2000,0000} \\ M \\ -P_{00N0,0000} \end{pmatrix},$$

395 to obtain the fixation probability of a single mutant, $u(N-1, 1, 0, 0)$, with the boundary
396 conditions: $u(N, 0, 0, 0) = 0$ and $u(0, 0, 0, 0) = u(0, 0, 0, 1) = \dots = u(0, 0, 0, N) = 1$. The
397 expected frequencies in the next generation in equation (G2) are replaced by equations (B1)
398 and (B5) when there is positive frequency-dependent selection due to reproductive isolation
399 and viability selection for the mutant.

400

401

402 **Appendix S8: The partial dominance model with two phenotypes**

403 Thus far we considered the model in which h is a parameter that determines the intermediate
404 phenotype of heterozygote (Appendix S1, S3). Here we consider the case where there are only
405 two phenotypes (A and a) and the heterozygous phenotype is A with probability h and a with
406 probability $1-h$. In this case, the mating probability between heterozygote ($Aa \times Aa$) is

$$407 \quad [h^2 + (1-h)^2 + 2h(1-h)(1-r)]y^2 = [1 - 2h(1-h)r]y^2. \quad (H1)$$

408 Therefore the frequencies after mating are

$$T\frac{\partial}{\partial x} x^2 + [1 - (1-h)r]xy + \frac{1}{4}[1 - 2h(1-h)r]y^2,$$

$$409 \quad T\frac{\partial}{\partial y} [1 - (1-h)r]xy + 2(1-r)xz + \frac{1}{2}[1 - 2h(1-h)r]y^2 + (1-hr)yz, \quad (H2)$$

$$T\frac{\partial}{\partial z} \frac{1}{4}[1 - 2h(1-h)r]y^2 + (1-hr)yz + z^2,$$

410 where $T = 1 - 2r(x + hy)[(1-h)y + z]$. This is the same as (A1) when $h = 0$ or 1 . By
 411 linearizing the dynamics (H2) after viability selection (A2) for small x and y , we have the
 412 same result as equation (3) in Appendix S1. The largest eigenvalue of the linearized system is
 413 $(1 + hs)(1 - hr)$, and the mutant can invade if and only if $(1 + hs)(1 - hr) > 1$. This condition
 414 ($s > r/(1 - hr)$) is the same as the original diploid model (Appendix S1).

415 For diffusion approximation analysis, we take the limit of weak fecundity and
 416 viability selections, $r \rightarrow 0$, $s \rightarrow 0$, and large population $N \rightarrow \infty$ with the products Nr and
 417 Ns being kept finite (Appendix S3). Assuming that both s and r are the order of ϵ , a small
 418 positive constant, the change in the allele frequency p of the mutant allele A is

$$419 \quad \Delta p = p(1-p)[-p + h(2p-1)]\left\{r[1 - 2p^2 - 4hp(1-p)] - s\right\} + O(\epsilon^2). \quad (H3)$$

420 Note that s in (H3) is the selection coefficient favoring the phenotype A. From (H3) we have
 421 the frequency dynamics:

$$422 \quad \dot{p} = p(1-p)[-p + h(2p-1)]\left\{r[1 - 2p^2 - 4hp(1-p)] - s\right\} \quad (H4)$$

423 When $h = 1/2$, this is a half of the haploid model (equation 8). The dynamics has two stable
 424 equilibria at $p = 0$ and $p = 1$, and an internal unstable equilibrium at

$$425 \quad p_c = \frac{h}{2h-1} - \frac{\sqrt{(2h^2 - 2h + 1)r + (2h-1)s}}{\sqrt{2r(2h-1)}} \quad \text{when } r > s. \quad \text{The relative fixation rate of a single}$$

426 mutant relative to that of a neutral mutant is given by $\phi = 2N\rho$:

$$427 \quad \phi = \frac{1}{\int_0^1 \exp\left\{\int_0^y [y + 2h(1-y)][R(1-y)(1-2hy+y) - S] dy\right\}}. \quad (H5)$$

428 where $R = 4Nr$ and $S = 4Ns$. As shown in Figure S3, the lowest fixation probability is
 429 obtained when $h = 1/2$. When $h = 1/2$, the fixation probability is exactly the same as the
 430 haploid model (Figs. 4G, 4H).

431 Exact fixation probabilities without approximation in small populations are also
 432 calculated as Appendix S6. Results are shown in Fig. 4B (the dotted dark-green line).

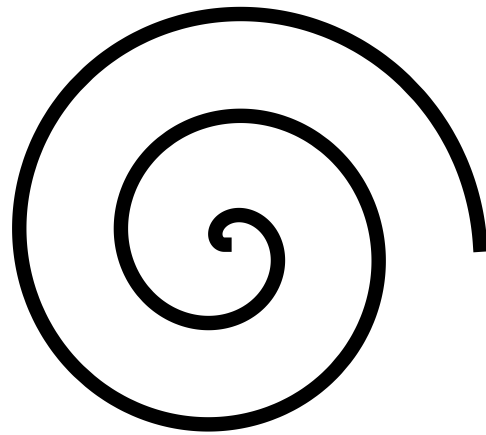
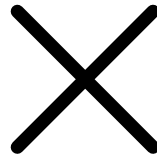
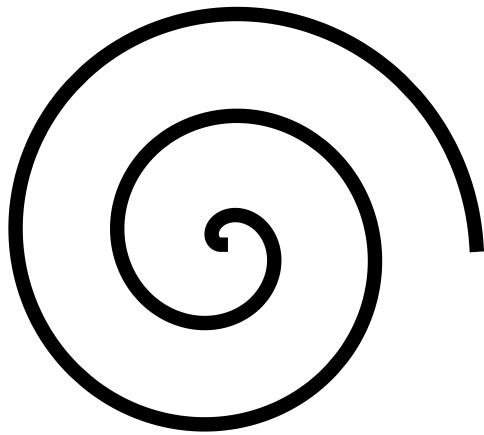
433

434

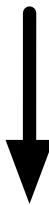
435 **Literature Cited**

- 436 Guckenheimer, J. and P. Holmes (1983) *Nonlinear Oscillations, Dynamical Systems, and*
437 *Bifurcations of Vector Fields*. Springer, New York
- 438 Nowak, M.A., Sasaki, A., Taylor, C., and Fudenberg, D. (2004) Emergence of cooperation
439 and evolutionary stability in finite populations. *Nature* 428: 646-650

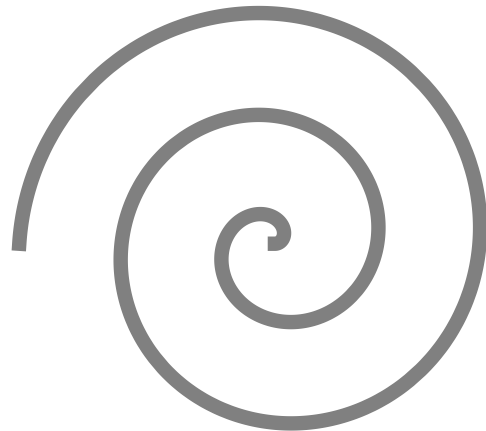
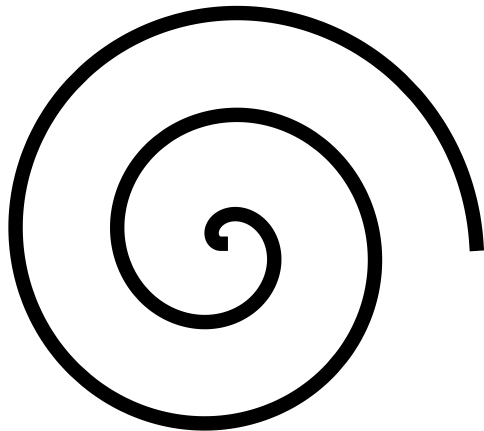
DD



SS

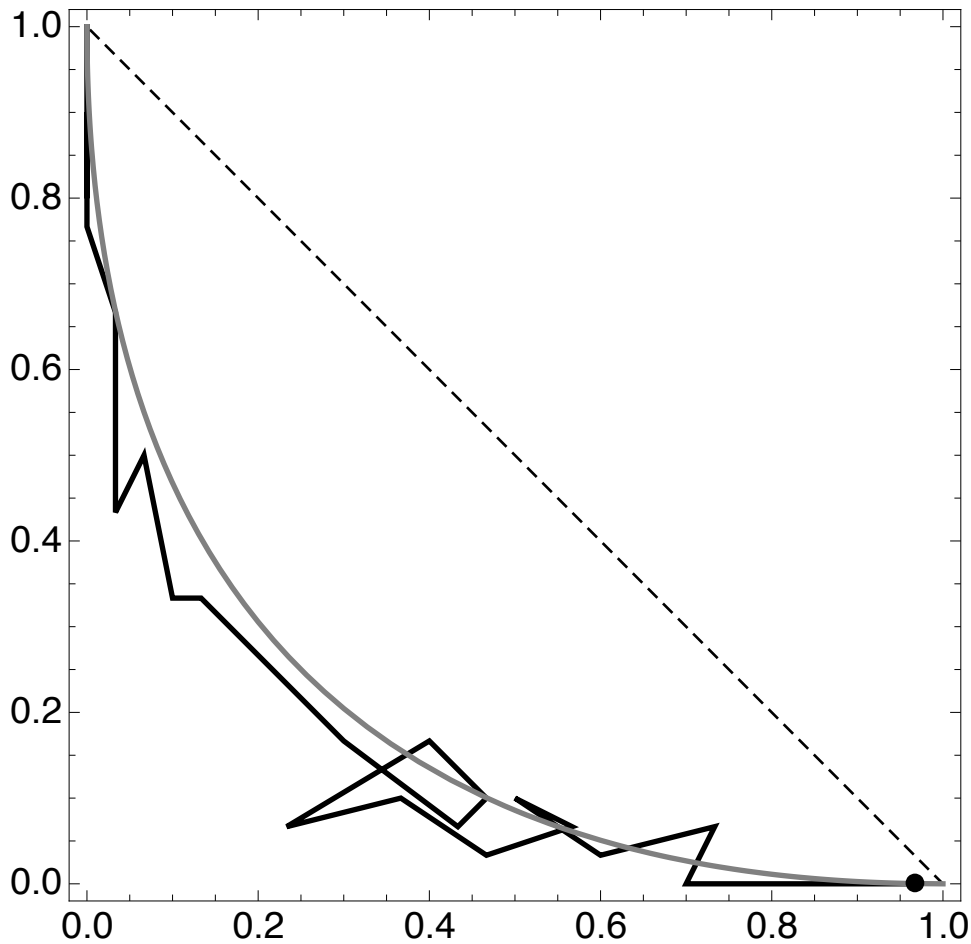


Ds

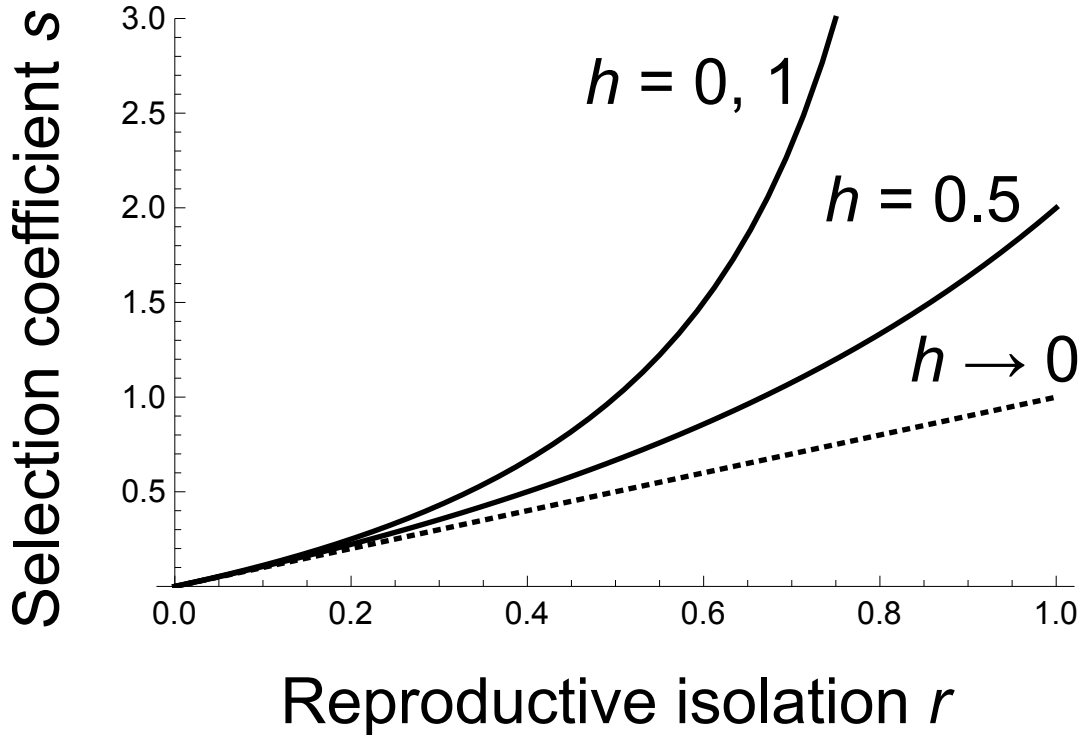


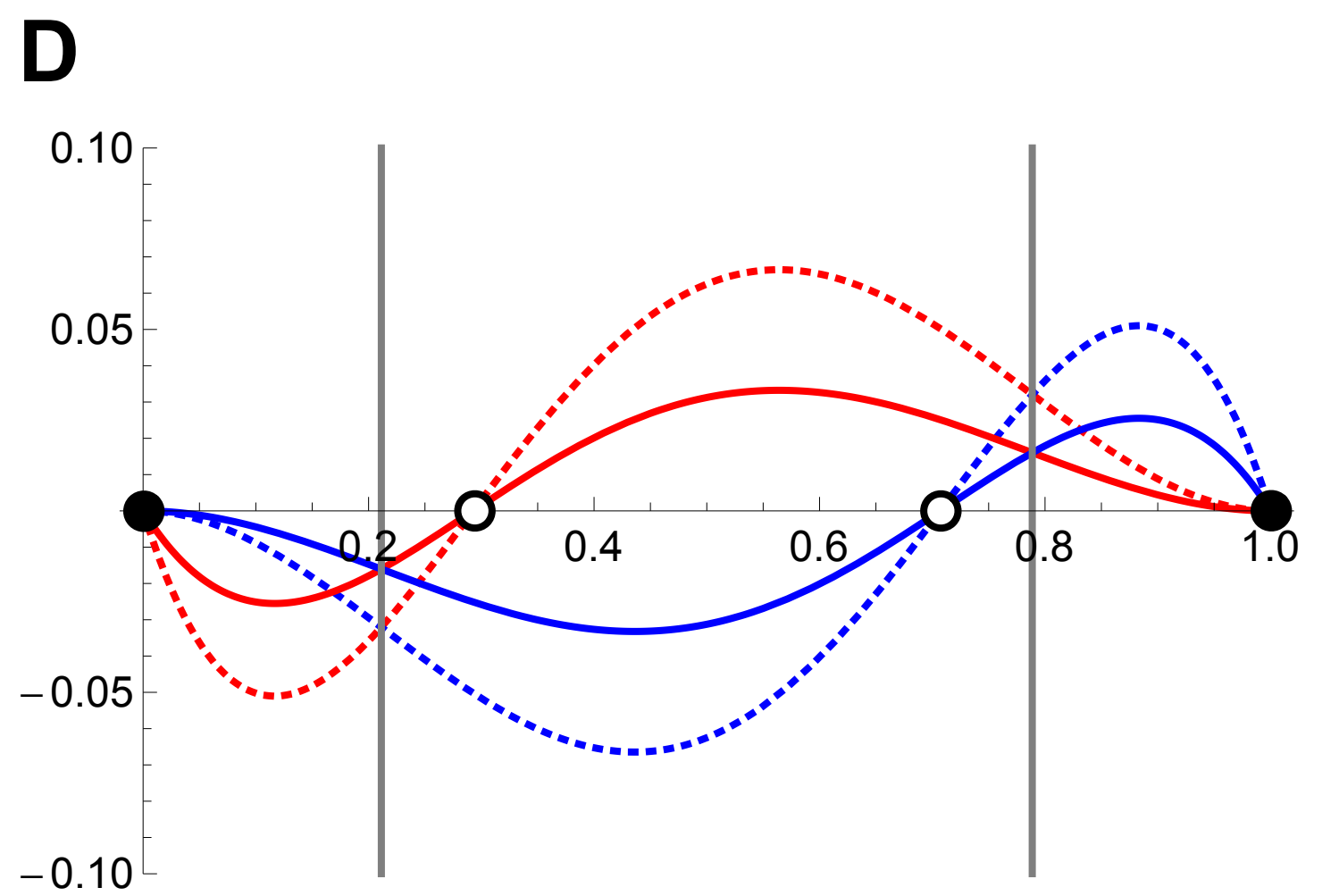
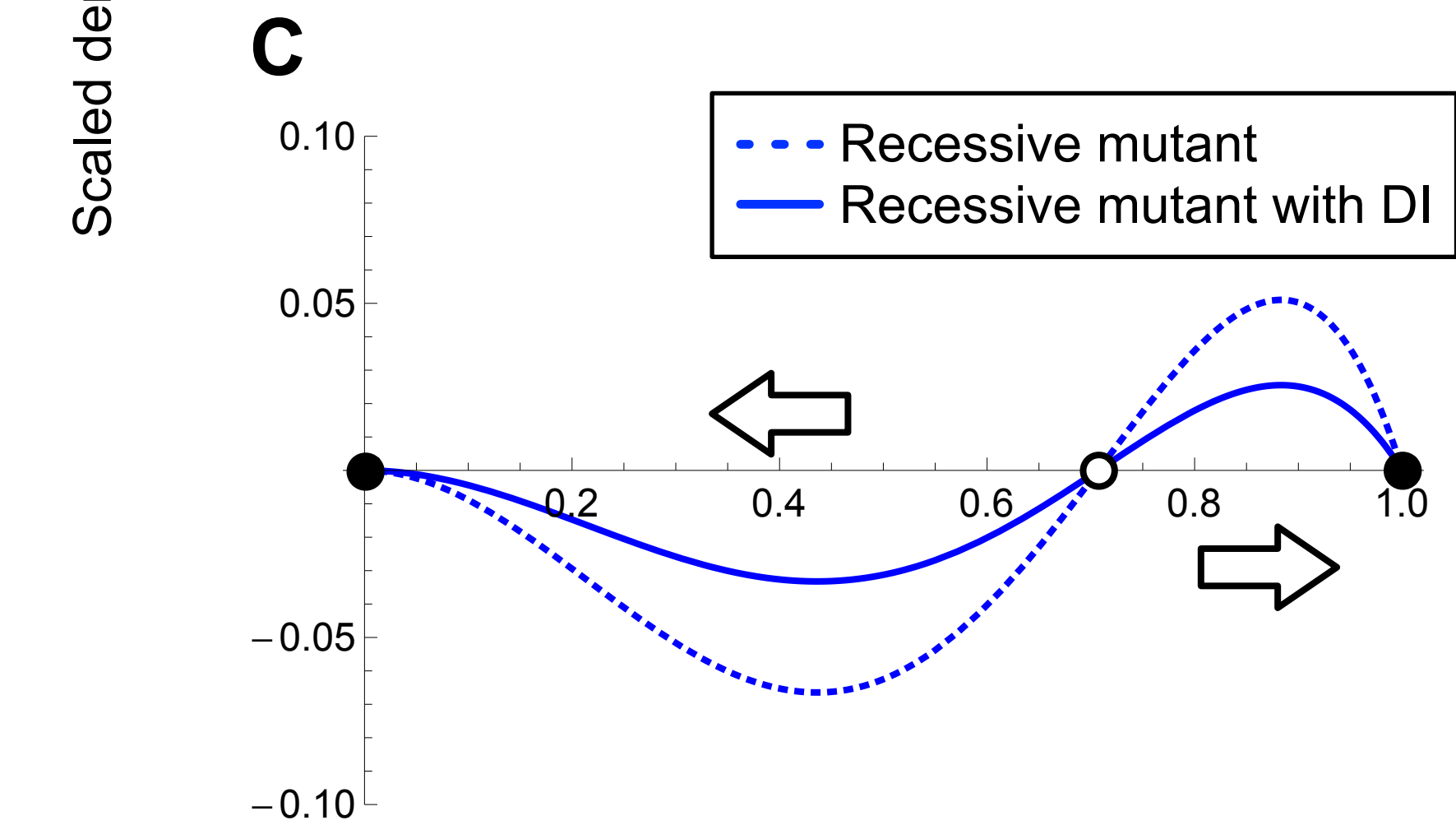
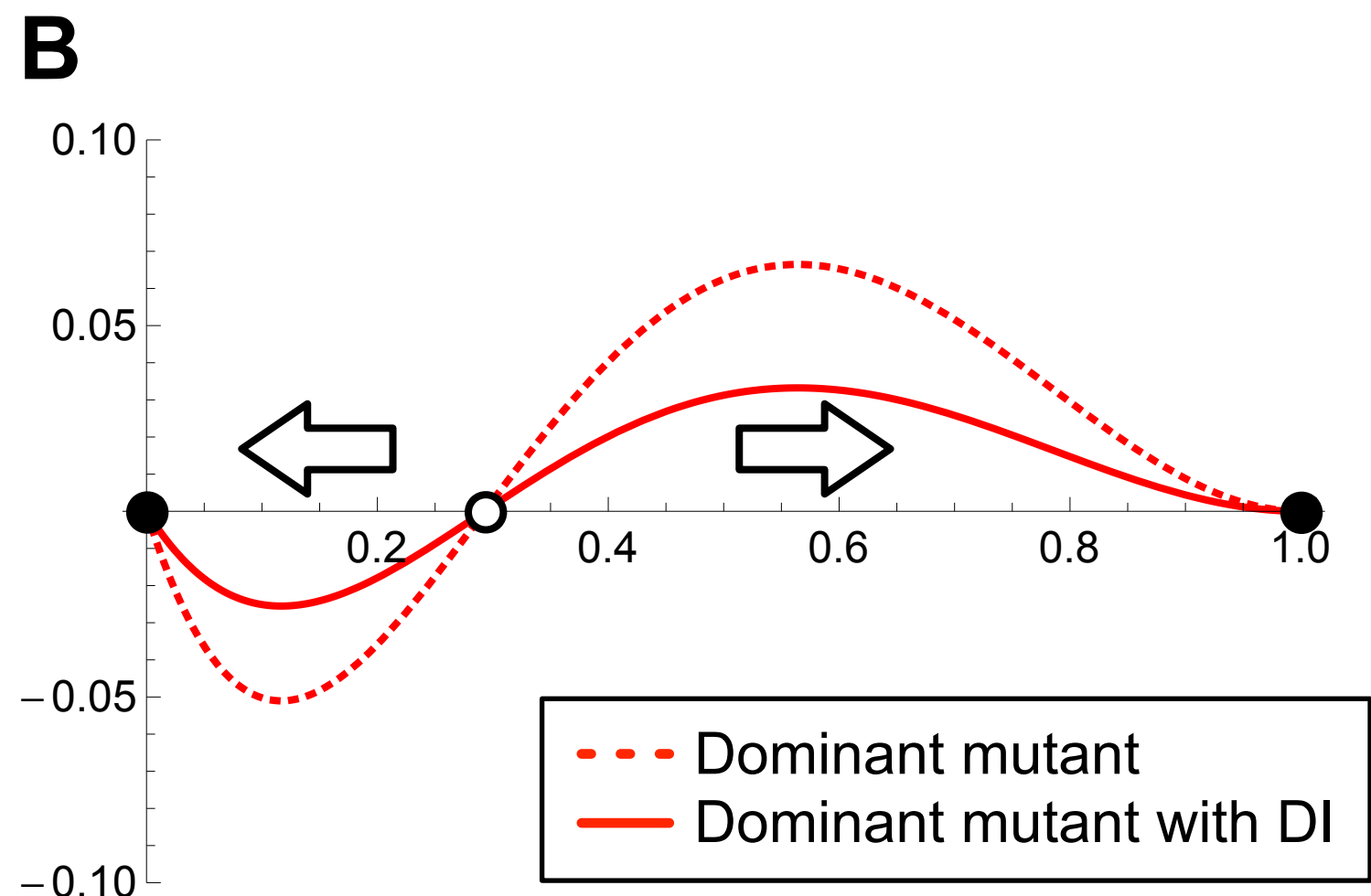
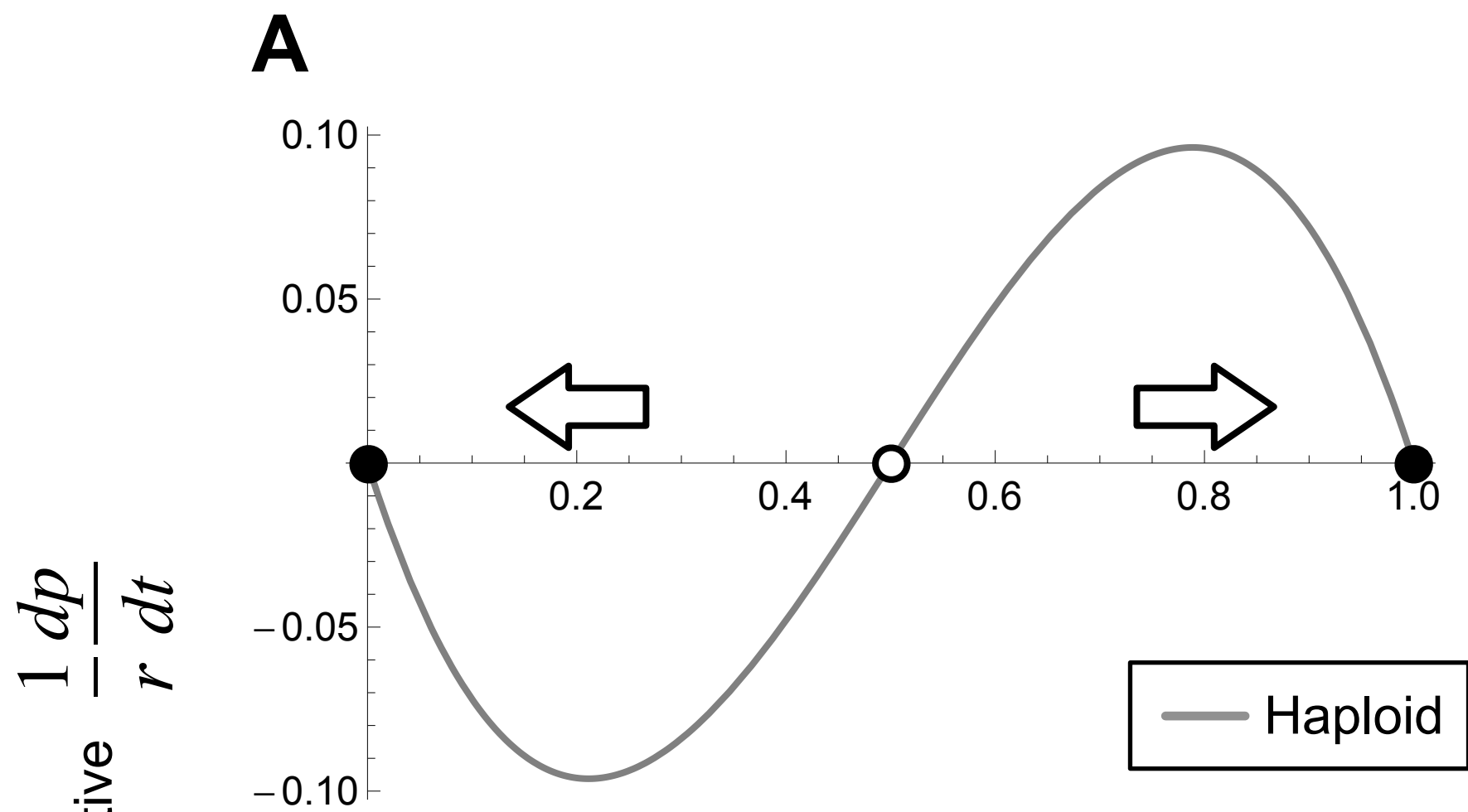
Ds

Mutant homozygote x



Resident homozygote z





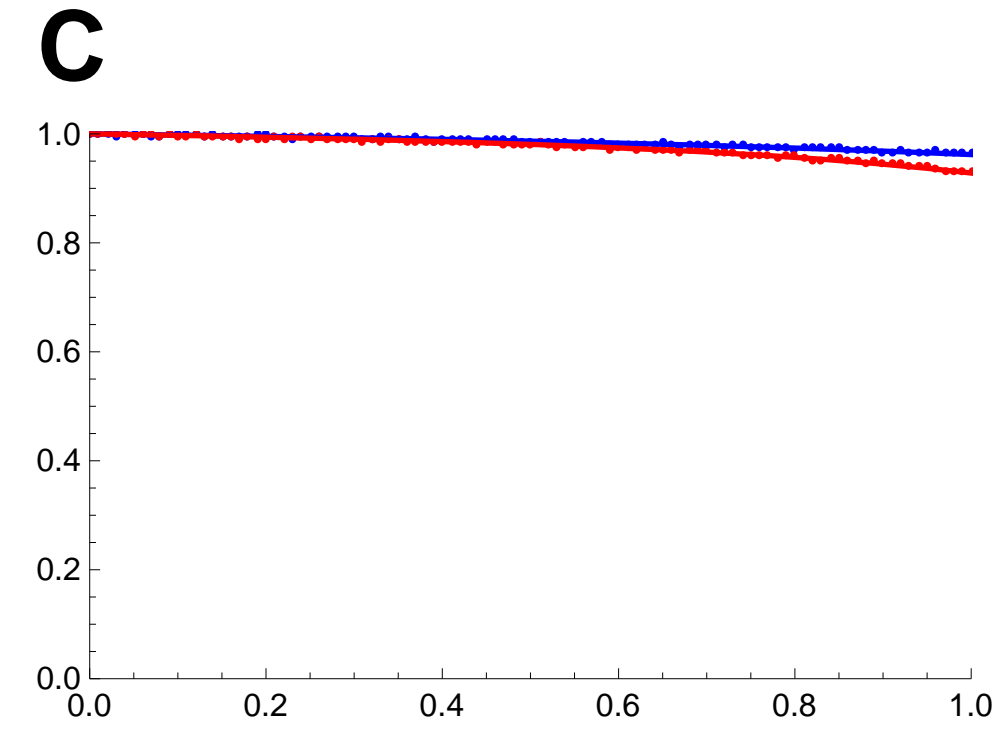
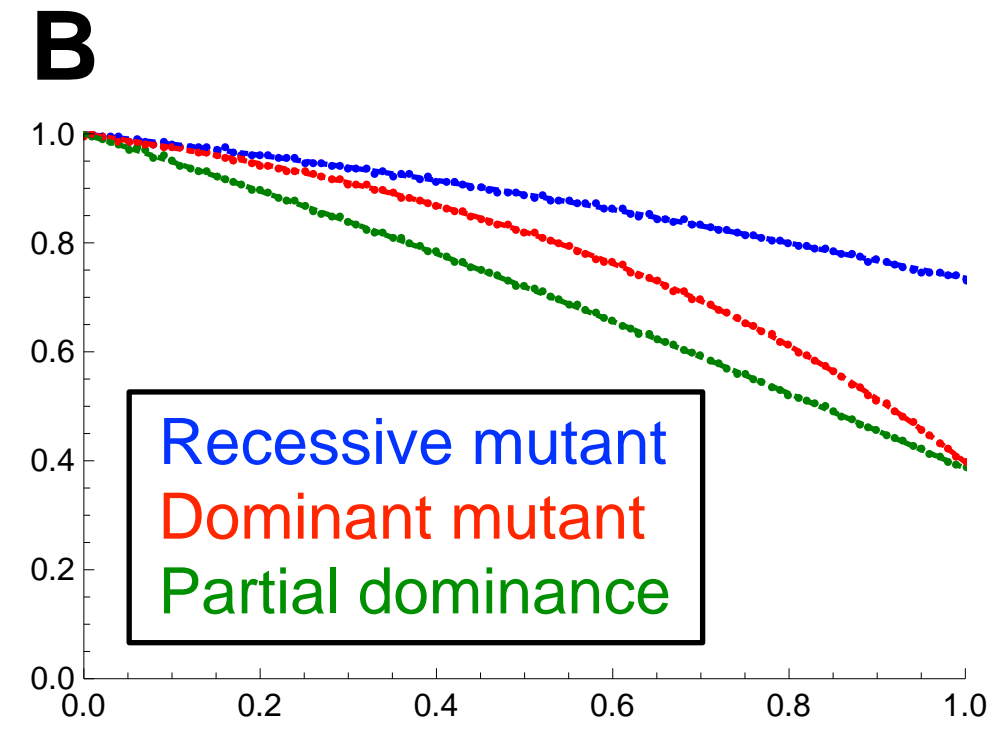
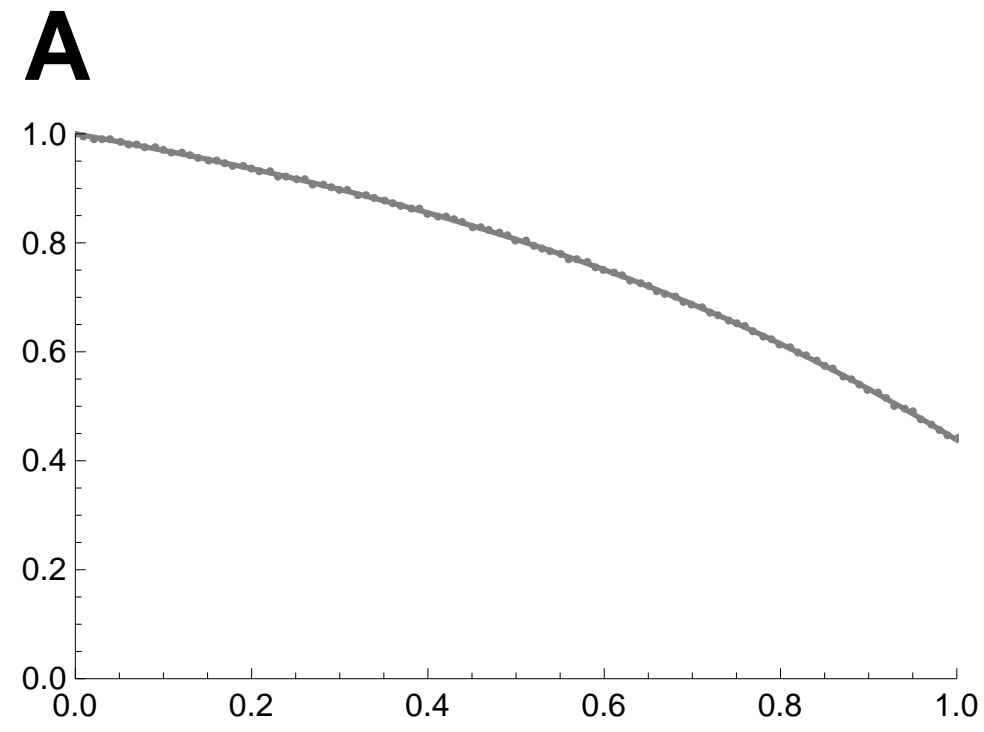
Mutant allele frequency p

Haploid

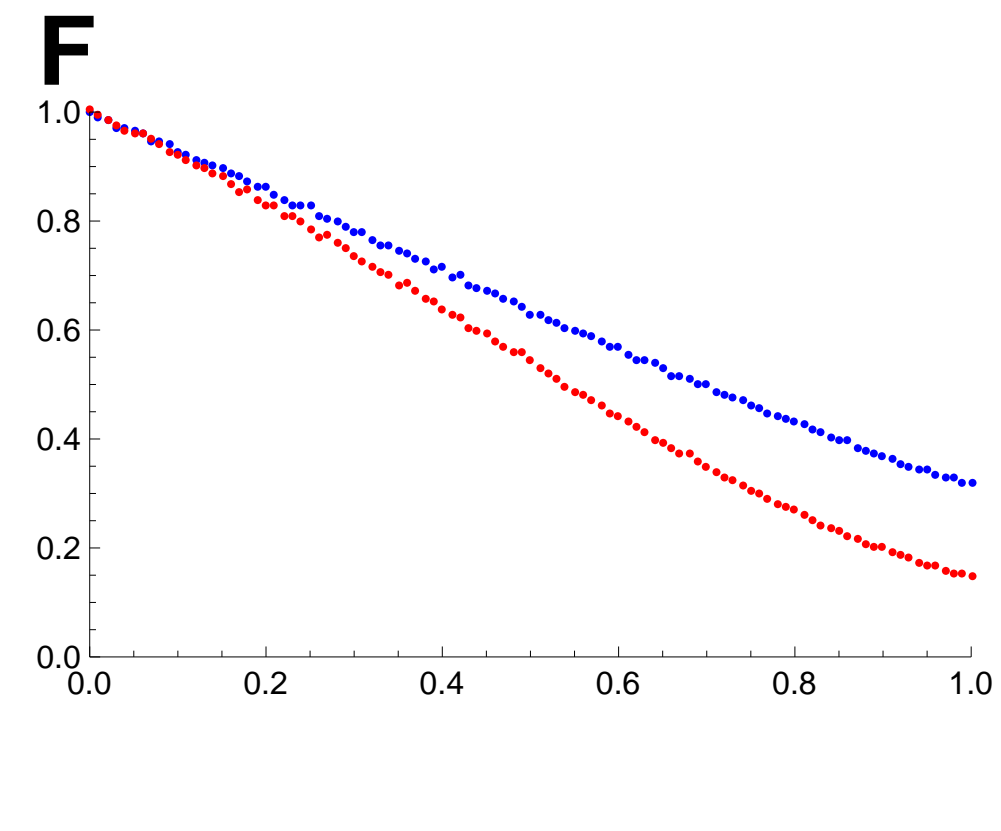
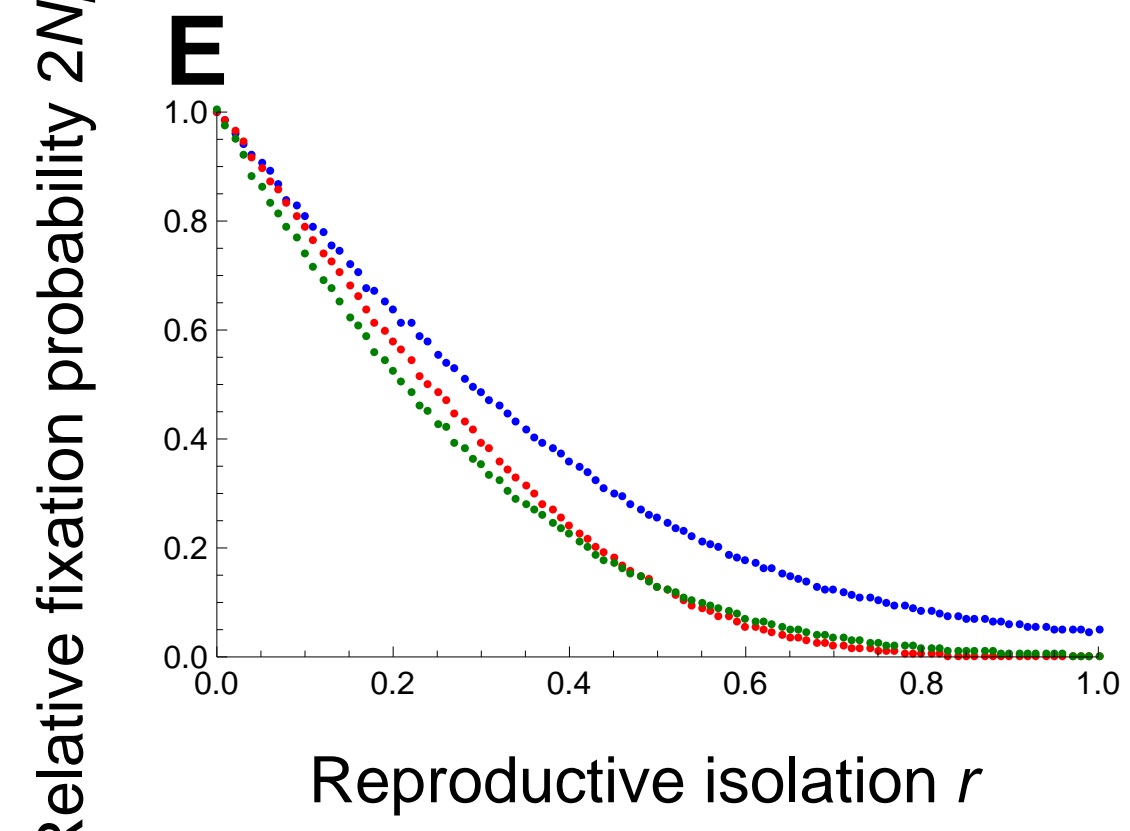
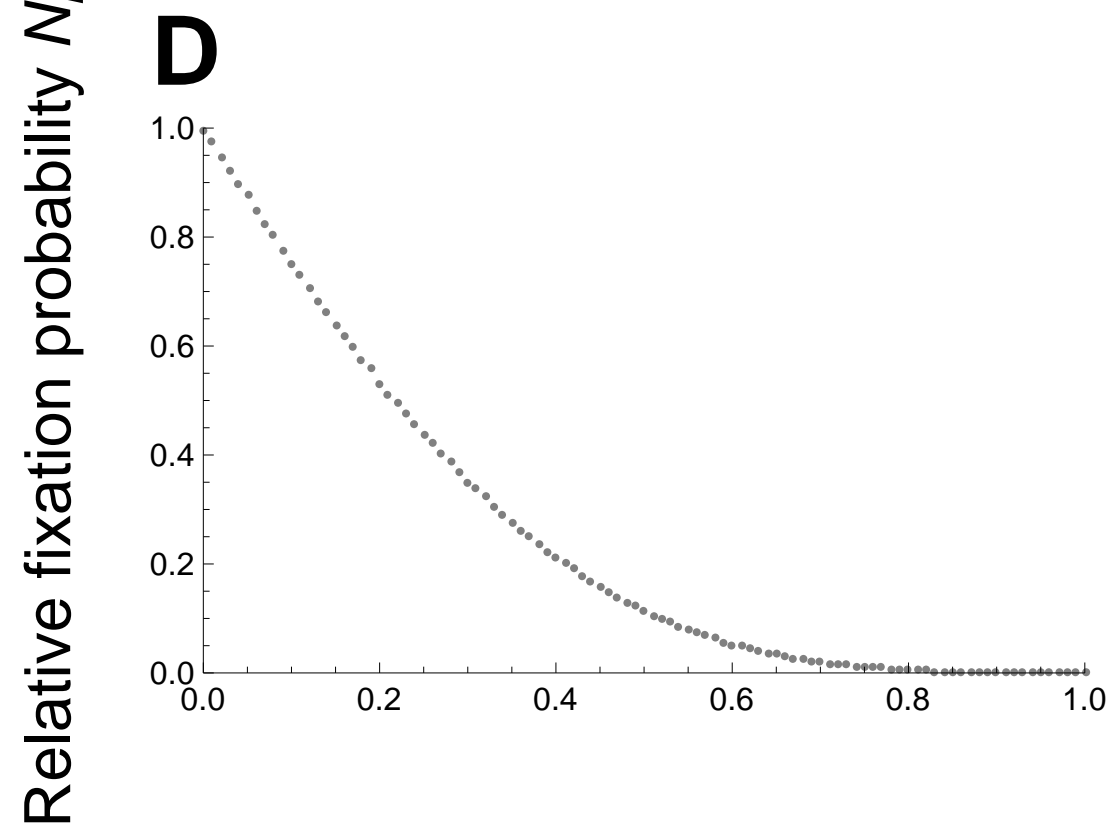
Diploid

Diploid with delayed inheritance

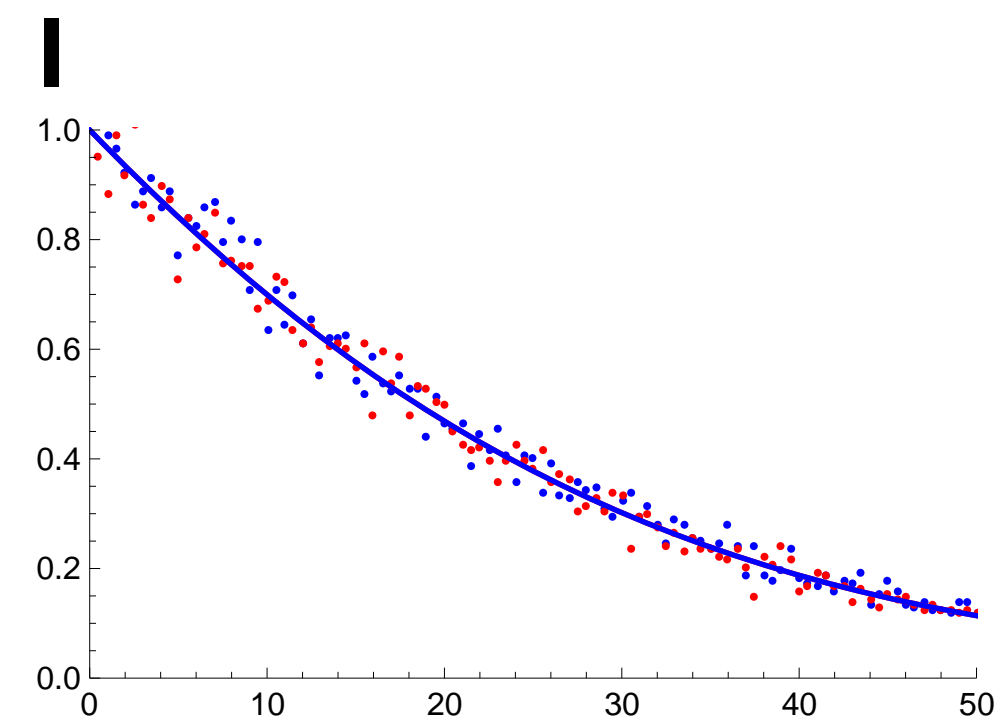
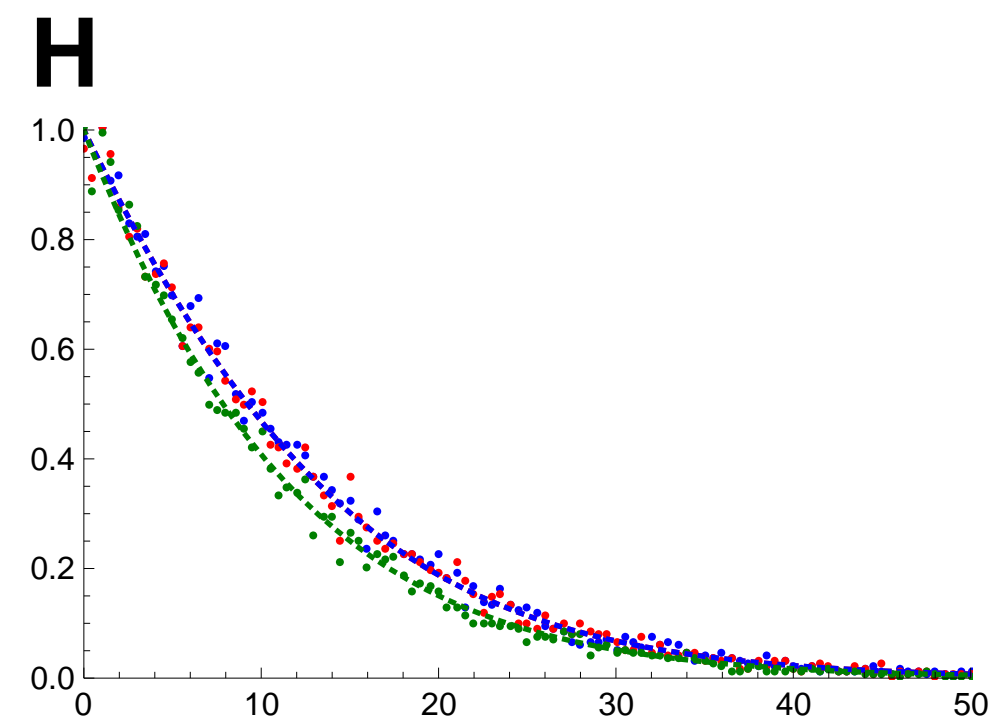
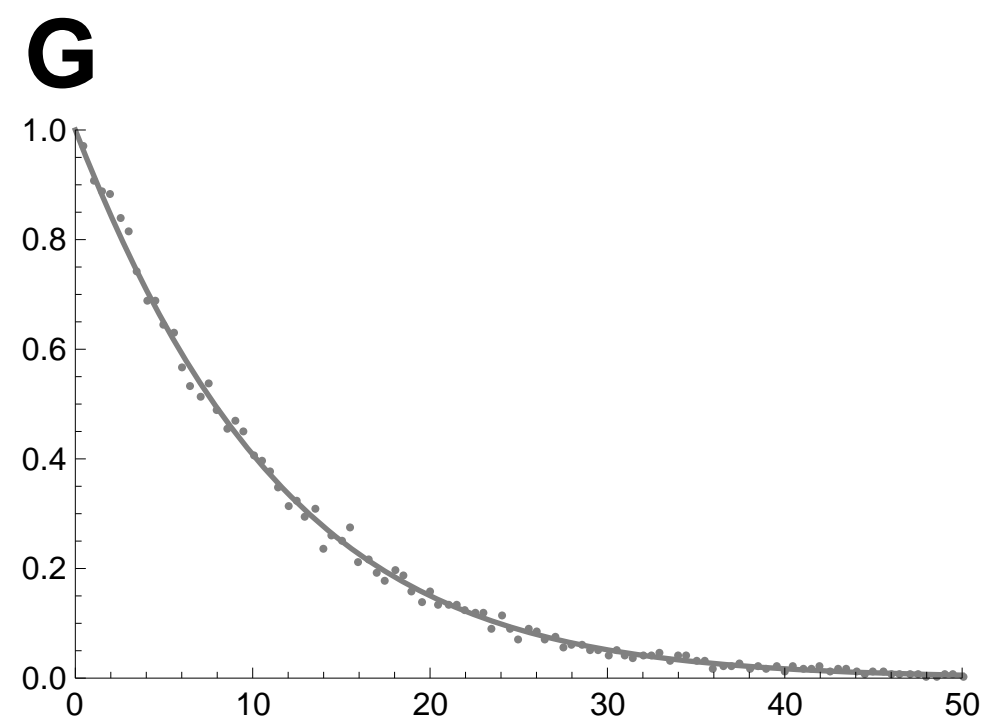
$N = 3$ (first step analysis
& simulation)

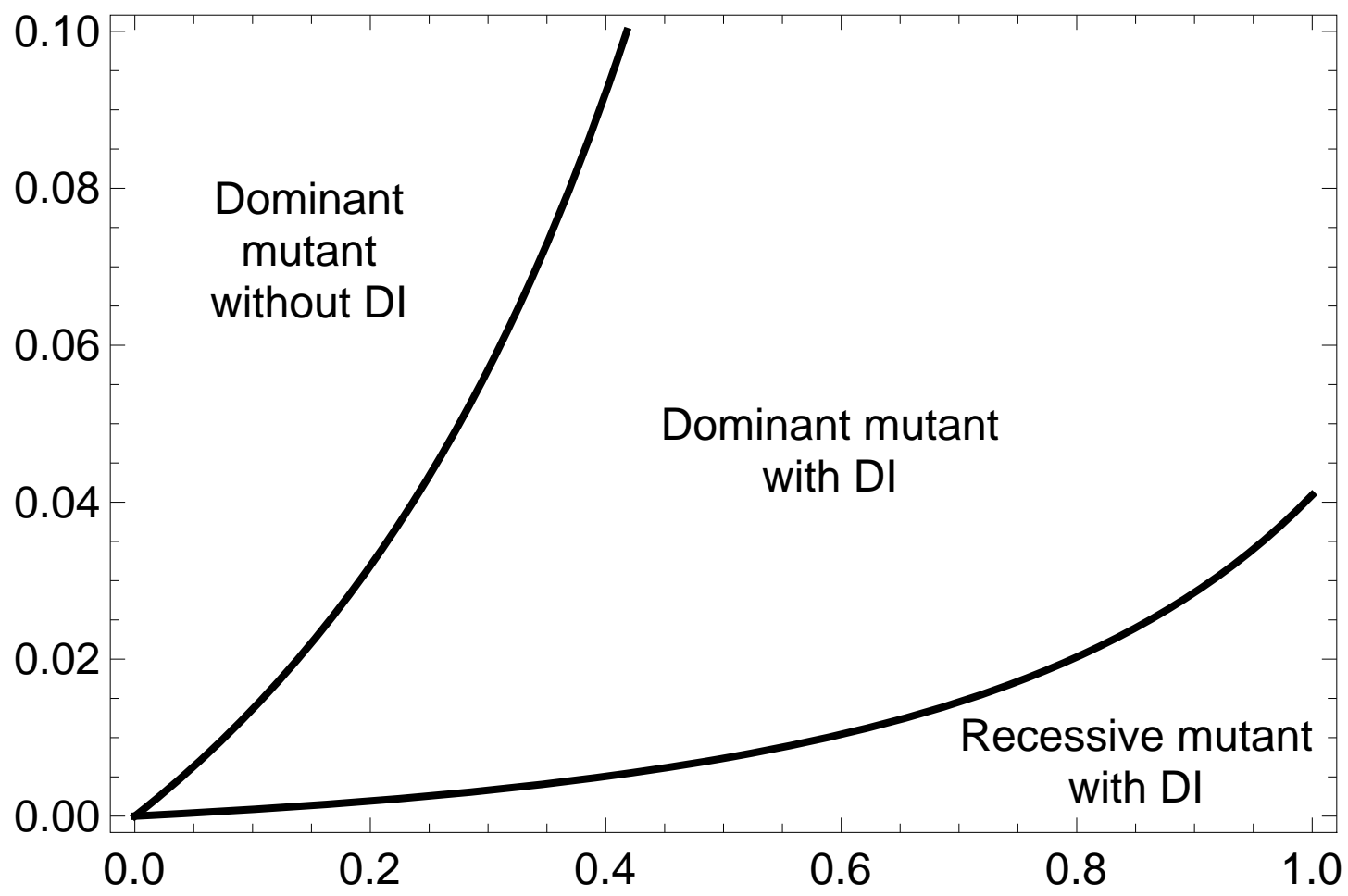
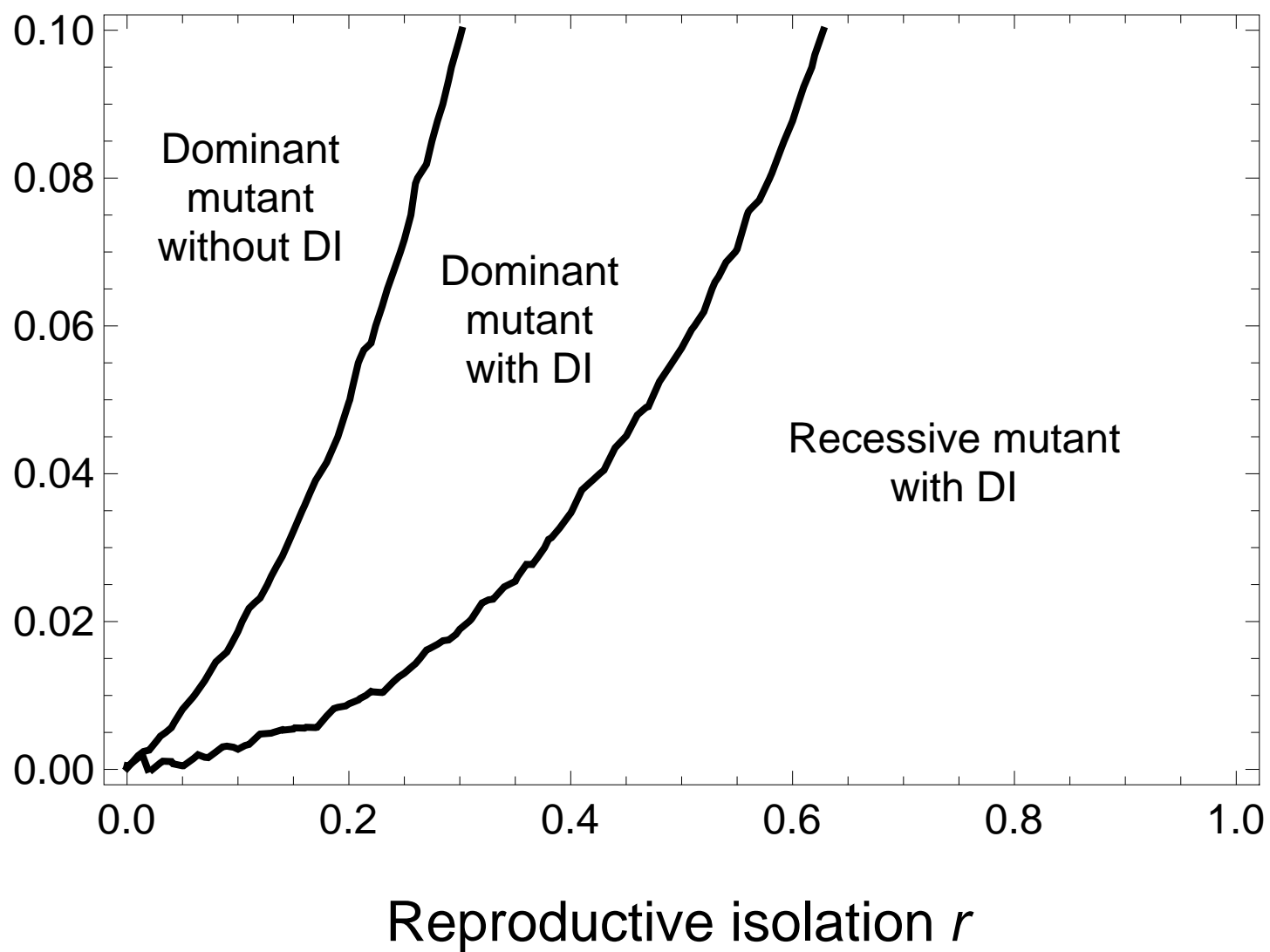
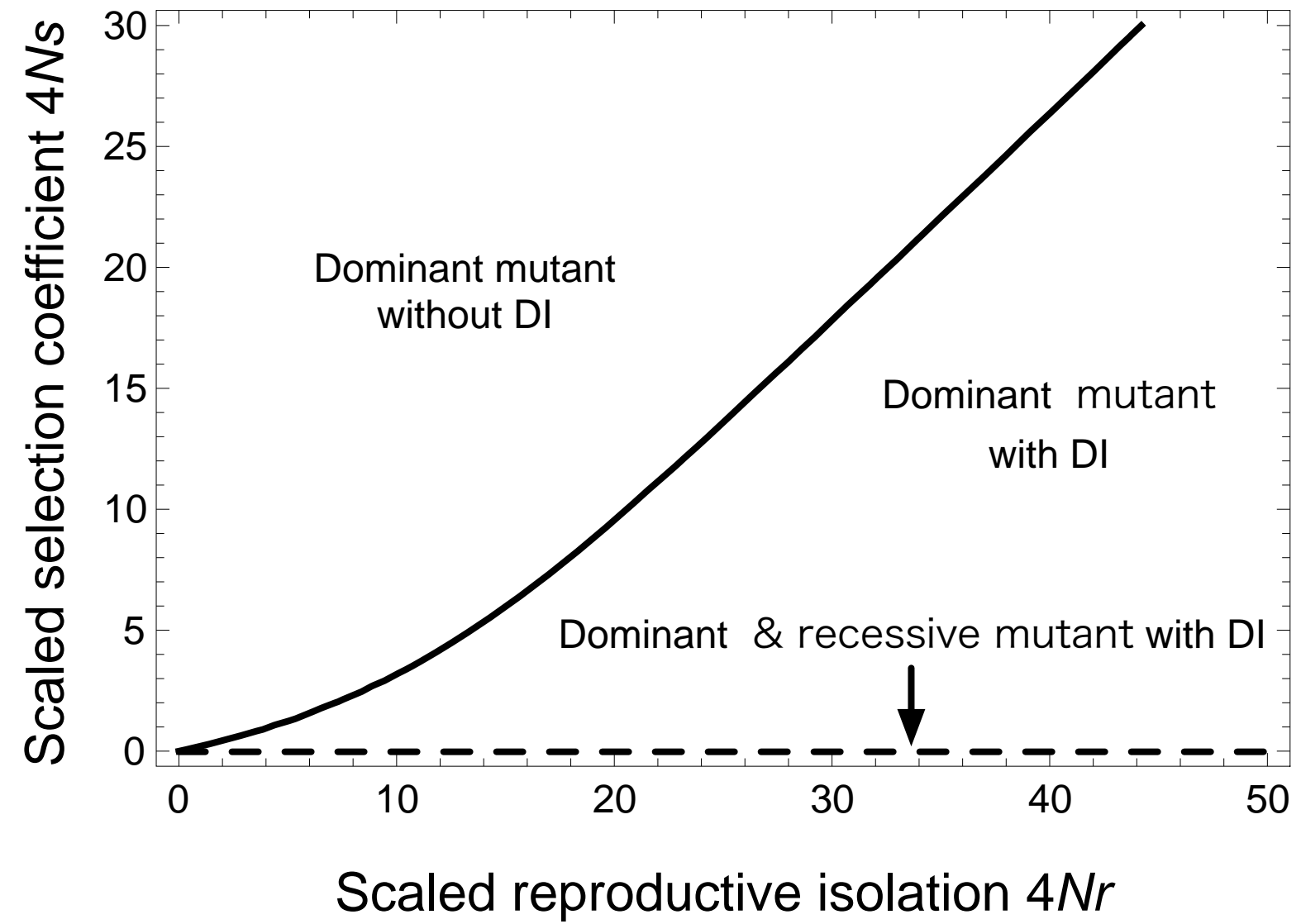


$N = 10$ (simulation)



$N \rightarrow \infty$ (diffusion approximation)
 $N = 1000$ (simulation)



A $N = 3$ (first step analysis)**B** $N = 10$ (simulation)**C** $N \rightarrow \infty$ (diffusion approximation)

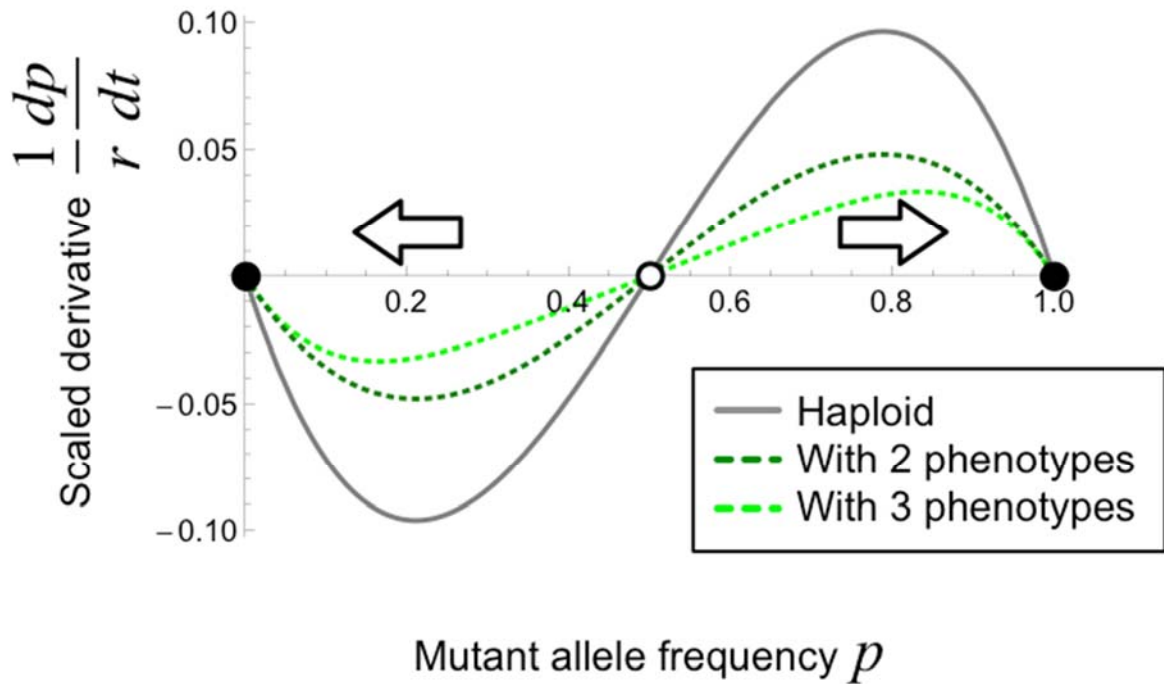


Figure S1: Allele frequency dynamics affected by positive frequency-dependent selection due to reproductive isolation (indicated by white arrows). *X*-axis: the mutant allele frequency (p). *Y*-axis: scaled derivatives of the mutant allele (\dot{p}/r). The haploid model (the solid gray line, eq. 8 when $s = 0$), the partial dominance model with two phenotypes (the dotted dark-green line, eq. H5 when $s = 0$ and $h = 1/2$), and the partial dominance model with three phenotypes (the dotted lime-green line, eq. 10 when $s = 0$ and $h = 1/2$). An unstable equilibrium at $p = 1/2$ (the white point) divides two basins of attraction. Stable equilibria are at $p = 0$ and 1 (the black points).

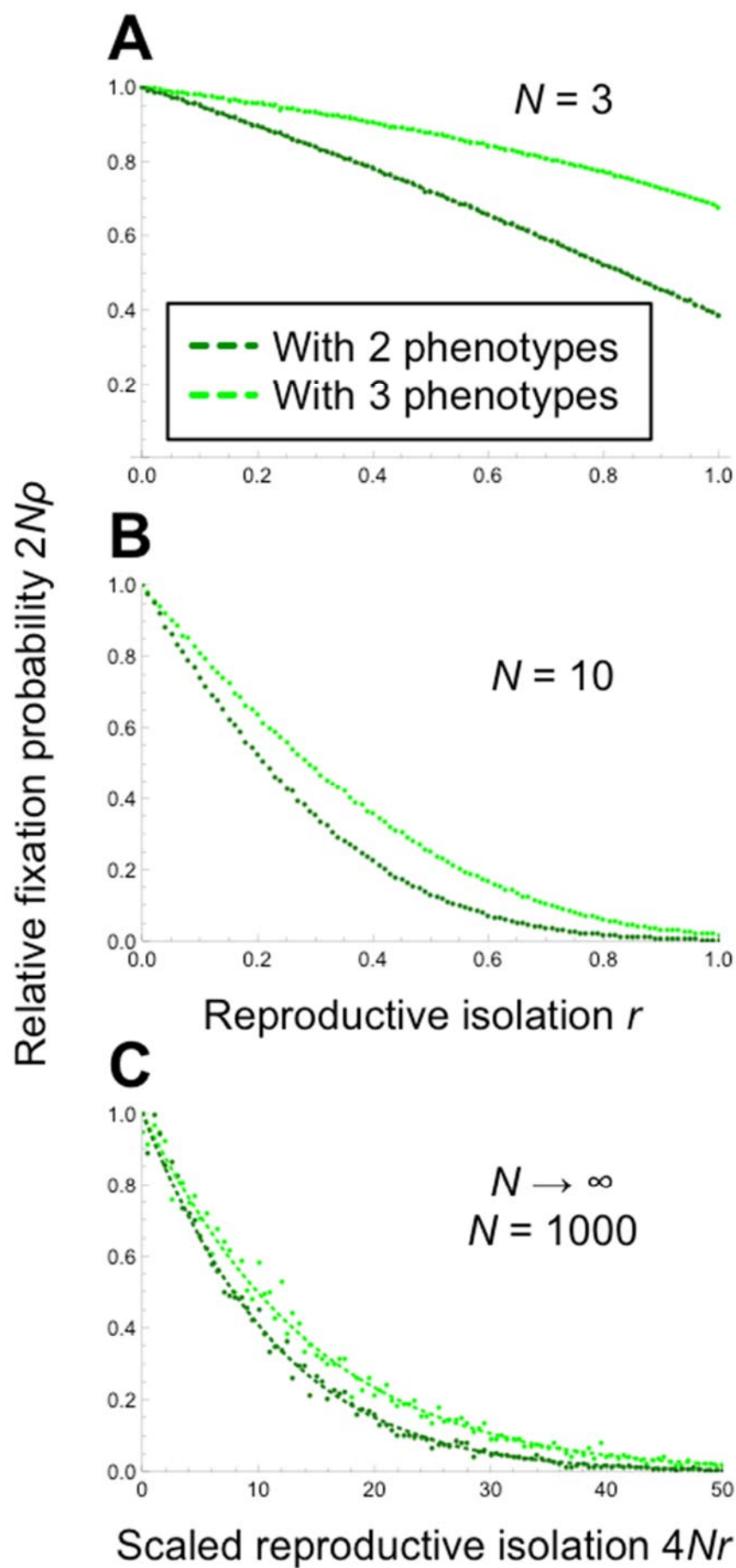


Figure S2: Relative fixation probabilities of a single mutant with reproductive isolation (and without viability selection: $s = 0$) to that of a neutral mutant. A, B: X -axis is the reproductive isolation parameter (r). C: X -axis is four times the product of the reproductive isolation parameter and the effective population size ($4Nr$). Y -axis is the product of fixation probability and effective population size ($2N\rho$). A: $N = 3$ (the first step analysis and Monte Carlo simulations), C: $N = 10$ (Monte Carlo simulations), C: $N \rightarrow \infty$ (diffusion approximation) and $N = 1000$ (Monte Carlo simulations). Dotted dark-green lines: the partial dominance model with two phenotypes. Dotted lime-green lines: the partial dominance model with three phenotypes.

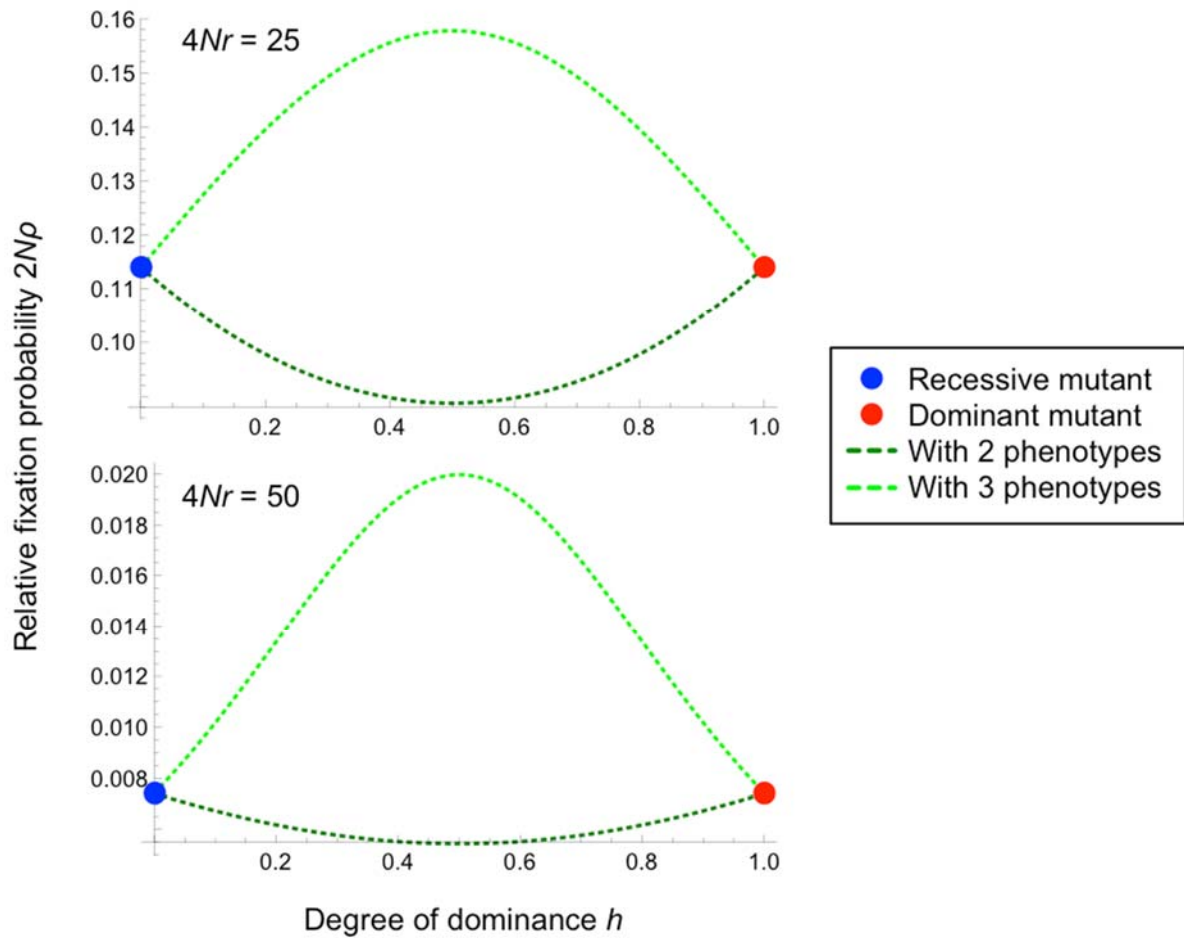


Figure S3: Effects of partial dominance in the diploid model without delayed inheritance in large populations. Blue points: the recessive mutant ($h = 0$). Red points: the dominant mutant ($h = 1$). Dotted dark-green lines: the partial dominance model with two phenotypes. Dotted lime-green lines: the partial dominance model with three phenotypes. When $R (= 4Nr) = 0$, the fixation probability is 1 regardless of h values.

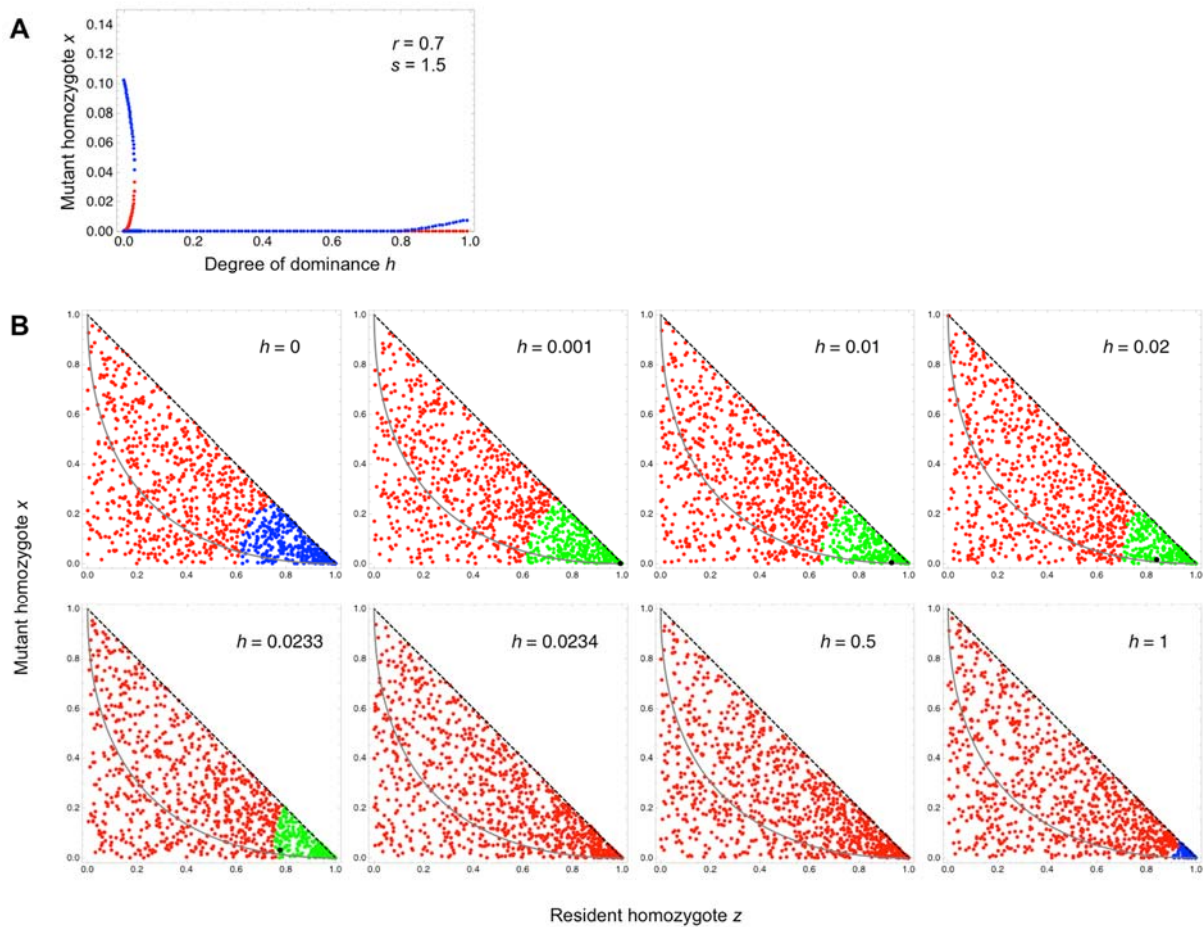


Figure S4: A: The bifurcation plot along the degree of dominance parameter (h). Y-axis is the frequency of the mutant homozygote (x). Red points: stable equilibria. Blue points: unstable equilibria. B: Simulation results of deterministic recursion equations (3)-(4). Red points: basin of attraction toward a stable equilibrium of the mutant allele. Blue points: basin of attraction toward a stable equilibrium of the resident allele. Green points: basin of attraction toward a stable equilibrium of both the mutant and resident alleles. The coexistence equilibria are shown as black points. The parameter condition is $r = 0.7$ and $s = 1.5$.

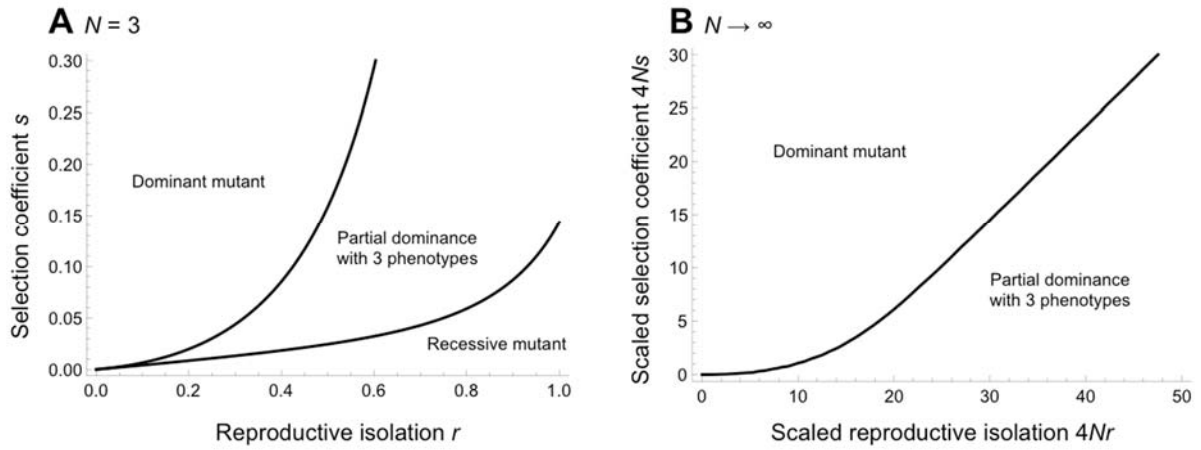


Figure S5: The alleles with the highest fixation probabilities in the diploid model without delayed inheritance given certain strength of reproductive isolation and viability selection. A: $N = 3$ (the first step analysis), B: $N \rightarrow \infty$ (diffusion approximation).

Table S1: The diploid model with delayed inheritance (when A is a dominant allele)

Mating comb.	Mating probability	AA _A				
AA _A ×AA _A	x_A^2	1	0	0	0	0
AA _A ×Aa _A	$2x_A y_A$	1/2	1/2	0	0	0
AA _A ×Aa _a	$2(1-r)x_A y_a$	1/2	1/2	0	0	0
AA _A ×aa _A	$2x_A z_A$	0	1/2	1/2	0	0
AA _A ×aa _a	$2(1-r)x_A z_a$	0	1/2	1/2	0	0
Aa _A ×Aa _A	y_A^2	1/4	1/2	0	1/4	0
Aa _A ×Aa _a	$2(1-r)y_A y_a$	1/4	1/2	0	1/4	0
Aa _A ×aa _A	$2y_A z_A$	0	1/4	1/4	1/4	1/4
Aa _A ×aa _a	$2(1-r)y_A z_a$	0	1/4	1/4	1/4	1/4
Aa _a ×Aa _A	y_a^2	1/4	1/2	0	1/4	0
Aa _a ×aa _A	$2(1-r)y_a z_A$	0	1/4	1/4	1/4	1/4
Aa _a ×aa _a	$2y_a z_a$	0	1/4	1/4	1/4	1/4
aa _A ×aa _A	z_A^2	0	0	0	0	1
aa _A ×aa _a	$2(1-r)z_A z_a$	0	0	0	0	1
aa _a ×aa _a	z_a^2	0	0	0	0	1